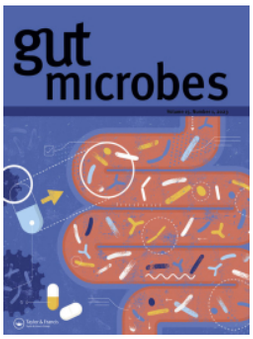

Gut Microbes

ISSN: 1949-0976 (Print) 1949-0984 (Online) Journal homepage: www.tandfonline.com/journals/kgmi20

Discovery and characterization of antitumor gut microbiota from amphibians and reptiles: *Ewingella americana* as a novel therapeutic agent with dual cytotoxic and immunomodulatory properties

Seigo Iwata , Nagi Yamasita , Kensuke Asukabe , Matomo Sakari & Eijiro Miyako

To cite this article: Seigo Iwata , Nagi Yamasita , Kensuke Asukabe , Matomo Sakari & Eijiro Miyako (2025) Discovery and characterization of antitumor gut microbiota from amphibians and reptiles: ***Ewingella americana*** as a novel therapeutic agent with dual cytotoxic and immunomodulatory properties, Gut Microbes, 17:1, 2599562, DOI: 10.1080/19490976.2025.2599562

To link to this article: https://doi.org/10.1080/19490976.2025.2599562

© 2025 The Author(s). Published with license by Taylor & Francis Group, LLC.

View supplementary material

Published online: 10 Dec 2025.

Submit your article to this journal

Article views: 83763

View related articles

View Crossmark data

Full Terms & Conditions of access and use can be found at
https://www.tandfonline.com/action/journalInformation?journalCode=kgmi20

GUT MICROBES
2025, VOL. 17, NO. 1, 2599562
https://doi.org/10.1080/19490976.2025.2599562

Taylor & Francis
Taylor & Francis Group

RESEARCH ARTICLE

OPEN ACCESS Check for updates

Discovery and characterization of antitumor gut microbiota from amphibians and reptiles: *Ewingella americana* as a novel therapeutic agent with dual cytotoxic and immunomodulatory properties

Seigo Iwata, Nagi Yamasita[§], Kensuke Asukabe[§], Matomo Sakari and Eijiro Miyako

Graduate School of Advanced Science and Technology, Japan Advanced Institute of Science and Technology, 1-1 Asahidai, Nomi, Ishikawa, Japan

ABSTRACT

The utilization of gut microbiota in cancer therapy has attracted considerable attention as an emerging therapeutic frontier. In this study, we systematically evaluated the antitumor effects of nine bacterial strains isolated from the intestines of amphibians (*Dryophytes japonicus* and *Cynops pyrrhogaster*) and a reptile (*Takydromus tachydromoides*). Among the isolates, *Ewingella americana* exhibited remarkably potent cytotoxic activity with selective tumor-targeting ability characteristic of facultative anaerobic bacteria. Mechanistic investigations revealed that *E. americana* functions through a dual-action mechanism: direct tumor cell killing and robust activation of host immunity, leading to enhanced T cell, neutrophil, and B cell-mediated tumor attack. Treatment with *E. americana* significantly outperformed standard therapies, including anti-PD-L1 antibody and doxorubicin, in tumor regression studies. Importantly, comprehensive safety evaluations in murine models demonstrated that the gut-derived *E. americana* strain exhibits minimal pathogenicity and exerts no significant adverse effects at therapeutically effective doses, contrasting favorably with genetically modified bacterial therapeutics. Comparative analysis revealed superior therapeutic efficacy of *E. americana* over conventional treatments while maintaining an excellent safety profile. These findings suggest that gut microbiomes of lower vertebrates harbor numerous uncharacterized bacterial species with exceptional therapeutic potential. Our study establishes a foundation for developing naturally occurring, non-pathogenic bacterial therapeutics and underscores the critical importance of microbial biodiversity in advancing cancer treatment strategies.

ARTICLE HISTORY
Received 2 September 2025
Revised 24 November 2025
Accepted 1 December 2025

KEYWORDS
Gut microbiota; cancer; bacterial cancer therapy; immunotherapy

Introduction

The landscape of cancer therapeutics has been revolutionized by the recognition that microbial communities play pivotal roles in tumor biology, therapeutic responses, and clinical outcomes. Research and development of bacterial therapies for cancer have been rapidly expanding, driven by accumulating evidence of the profound interconnections between the microbiome and oncological processes. In the human body, microbial ecosystems establish complex communities across diverse anatomical niches, including the respiratory tract, integumentary system, oral cavity, urogenital tract, and most prominently, the gastrointestinal tract, each harboring distinct and highly diverse microbial species assemblages.[1] Among these microbiomes, the gut microbiota has emerged as the most extensively characterized and therapeutically relevant, comprising a dense and intricate ecosystem of commensal microorganisms that collectively outnumber human cells and encode a metabolic capacity far exceeding that of the human genome.[1,2]

The gut microbiome plays multifaceted roles in maintaining physiological homeostasis, with its functions extending far beyond traditional concepts of microbial residence. Specifically, the gut microbiota serves as a critical mediator of digestive processes and metabolic regulation, orchestrates sophisticated

CONTACT Eijiro Miyako e-miyako@jaist.ac.jp Graduate School of Advanced Science and Technology, Japan Advanced Institute of Science and Technology, 1-1 Asahidai, Nomi, Ishikawa 923-1292, Japan
[§]N. Y. and K. A. contributed equally.
Supplemental data for this article can be accessed online at https://doi.org/10.1080/19490976.2025.2599562.

© 2025 The Author(s). Published with license by Taylor & Francis Group, LLC.
This is an Open Access article distributed under the terms of the Creative Commons Attribution-NonCommercial License (http://creativecommons.org/licenses/by-nc/4.0/), which permits unrestricted non-commercial use, distribution, and reproduction in any medium, provided the original work is properly cited. The terms on which this article has been published allow the posting of the Accepted Manuscript in a repository by the author(s) or with their consent.

immune system modulation, and provides essential defense mechanisms against pathogenic invasion.[3-5] The metabolic versatility of gut bacteria enables the production of numerous bioactive compounds, including short-chain fatty acids, secondary bile acids, and complex metabolites that profoundly influence host physiology and disease susceptibility. Furthermore, the gut microbiome serves as a primary site for immune system education and calibration, with microbial-derived signals shaping both local intestinal immunity and systemic immune responses throughout the host organism.

Accumulating evidence has established compelling associations between gut microbiota composition and cancer biology, demonstrating that specific bacterial species can significantly influence cancer initiation, progression trajectories,[6-9] and therapeutic responses across multiple cancer types.[6,10,11] The mechanisms underlying these microbiome-cancer interactions are remarkably diverse, encompassing direct genotoxic effects, chronic inflammatory processes, immune system modulation, and metabolic reprogramming of the tumor microenvironment. For instance, pioneering studies have identified specific gut microbial species that substantially enhance the therapeutic efficacy of immune checkpoint inhibitors, including programmed cell death-1 (PD-1) inhibitors (anti-PD-1 antibodies) and programmed cell death ligand-1 (PD-L1) inhibitors (anti-PD-L1 antibodies), through mechanisms involving enhanced antigen presentation, T cell priming, and reversal of immunosuppressive tumor microenvironments.[12-14] These discoveries have catalyzed intense interest in developing microbiome-based therapeutic interventions and have established the gut microbiome as a critical determinant of immunotherapy responsiveness.

However, despite these significant advances, there remains a substantial gap between our understanding of microbiome-cancer associations and the clinical translation of gut bacteria for direct cancer treatment applications. To date, there have been remarkably few reports describing the systematic isolation of gut bacteria and their subsequent intravenous administration for direct antitumor therapy, representing a significant unexplored therapeutic opportunity. Moreover, current knowledge encompasses only a limited fraction of the vast microbial diversity residing within gut ecosystems, with the majority of bacterial species remaining uncharacterized regarding their potential beneficial or detrimental effects on human health. This knowledge gap is particularly pronounced for microbiomes of non-human species, which may harbor unique bacterial communities with novel therapeutic properties.

Building upon our previous groundbreaking work on tumor-resident microbiota that exhibited exceptional antitumor effects,[15-17] we have developed an innovative therapeutic approach wherein bacteria isolated directly from tumor tissues are cultured and administered intravenously to exploit their intrinsic antitumor activities and natural tumor-homing capabilities. The scientific rationale for investigating gut microbiota as a source of antitumor bacteria is multifaceted and compelling. First, gut bacteria are known to exert profound influence on systemic immune responses and inflammatory processes through the gut-systemic axis, suggesting their potential for remote antitumor effects. Second, gut bacteria can undergo translocation into the systemic circulation and subsequently colonize tumor tissues, representing one of the primary sources of intratumoral bacterial communities. Third, the evolutionary pressure within the gut environment may have selected for bacterial strains with unique metabolic capabilities and host interaction properties that could be therapeutically exploited.

Based on these considerations, we hypothesize that the gut microbiome represents a vast reservoir of bacterial diversity, encompassing species with potentially exceptional antitumor properties that remain largely unexplored. However, the clinical translation of gut bacteria for systemic cancer therapy faces significant challenges, particularly regarding safety considerations when bacteria are administered directly into the bloodstream. The potential for bacterial toxicity, septic complications, and uncontrolled inflammatory responses represents major barriers to therapeutic implementation. Additionally, current cancer therapeutic approaches employing genetically engineered bacteria (*Escherichia coli*, *Listeria monocytogenes*, and *Salmonella* species) carry inherent safety risks associated with potential spontaneous mutations in the bacterial genome, which could compromise the engineered safety features and therapeutic efficacy.[18,19] These concerns have limited the clinical advancement of bacterial cancer therapeutics and highlight the critical need for safer alternative approaches.

One promising strategy to address these safety challenges involves the identification and utilization of naturally occurring, non-pathogenic bacterial strains that combine potent antitumor activity with minimal toxicity profiles. Such bacteria would obviate the need for genetic modification while potentially maintaining or exceeding the therapeutic efficacy of engineered strains. Furthermore, recent innovative studies

have demonstrated that simple scaffold-mediated bacterial culturing methods can significantly reduce bacterial toxicity and enhance biocompatibility,[20] thereby improving the feasibility and safety profile of bacterial therapeutic approaches. Additionally, the use of naturally occurring bacteria may provide advantages in terms of regulatory approval pathways and clinical translation timelines.[21]

The exploration of gut microbiomes from phylogenetically diverse vertebrate species represents an innovative approach to bacterial discovery that may yield bacterial strains with unique therapeutic properties. Lower vertebrates, including amphibians and reptiles, have evolved distinct gut microbial communities adapted to their specific ecological niches, dietary patterns, and physiological requirements. These microbiomes may harbor bacterial species with novel metabolic capabilities, antimicrobial activities, and host interaction mechanisms that differ substantially from those found in mammalian gut microbiomes. Furthermore, the evolutionary divergence of these host species may have resulted in the selection of bacterial strains with enhanced stability, reduced pathogenicity, and unique therapeutic properties.

In this comprehensive study, we systematically investigated the antitumor potential of nine naturally occurring bacterial strains isolated from the intestinal tracts of phylogenetically diverse amphibians, specifically the Japanese tree frog (*Dryophytes japonicus*) and the Japanese fire belly newt (*Cynops pyrrhogaster*), and the Japanese grass lizard (*Takydromus tachydromoides*), a representative reptile species. These species were selected based on their ecological diversity, distinct evolutionary lineages, and accessibility for microbiome sampling. Our comprehensive evaluation encompassed multiple therapeutic parameters, including direct cytotoxic effects, tumor specificity, immunomodulatory properties, and safety profiles. The therapeutic efficacy of identified bacterial candidates was rigorously compared with established cancer treatments, including immune checkpoint inhibition (anti-PD-L1 antibody) and conventional chemotherapy (doxorubicin). Additionally, we conducted extensive safety evaluations to assess the pathogenic potential and adverse effect profiles of the most promising bacterial isolates.

This study provides novel insights into the therapeutic potential of previously uncharacterized gut microbes from lower vertebrates and establishes a foundation for the development of naturally occurring bacterial therapeutics in cancer treatment. Our findings demonstrate the vast untapped potential residing within diverse microbial ecosystems and highlight the critical importance of biodiversity conservation efforts in advancing medical science and therapeutic innovation.

Results

Isolation and characterization of gut microbiota from amphibians and reptiles

The composition and diversity of gut microbiota exhibit remarkable variation across host species, with numerous factors including dietary patterns, environmental antigen exposure, infectious disease history, pharmacological interventions, genetic background, host age, and hygiene practices profoundly influencing microbial community structure and function.[22-24] Furthermore, phylogenetically distinct host species often harbor entirely unique and largely uncharacterized gut microbial communities that have co-evolved with their respective hosts over evolutionary timescales. The intricate host-microbiota interactions that emerge from these relationships play pivotal roles in determining health outcomes versus disease susceptibility. Of particular interest is the epidemiological observation that spontaneous tumor formation in wild amphibian populations occurs at remarkably low frequencies and is typically restricted to specific populations or species, contrasting markedly with neoplasm prevalence patterns observed in other vertebrate taxa.[25] This striking phenomenon suggests that amphibians may possess inherent resistance mechanisms against carcinogenesis, although the underlying molecular and cellular mechanisms responsible for this apparent cancer resistance remain incompletely elucidated and represent an area of significant scientific interest.[23]

In the present investigation, we systematically isolated gut bacteria from phylogenetically diverse lower vertebrates, including two amphibian species (*Dryophytes japonicus* and *Cynops pyrrhogaster*) and one reptilian species (*Takydromus tachydromoides*). Figure 1a provides a comprehensive schematic illustration of the bacterial isolation methodology employed for amphibian and reptilian gut microbiota sampling. Through systematic cultivation and isolation protocols, a total of 45 distinct bacterial strains were

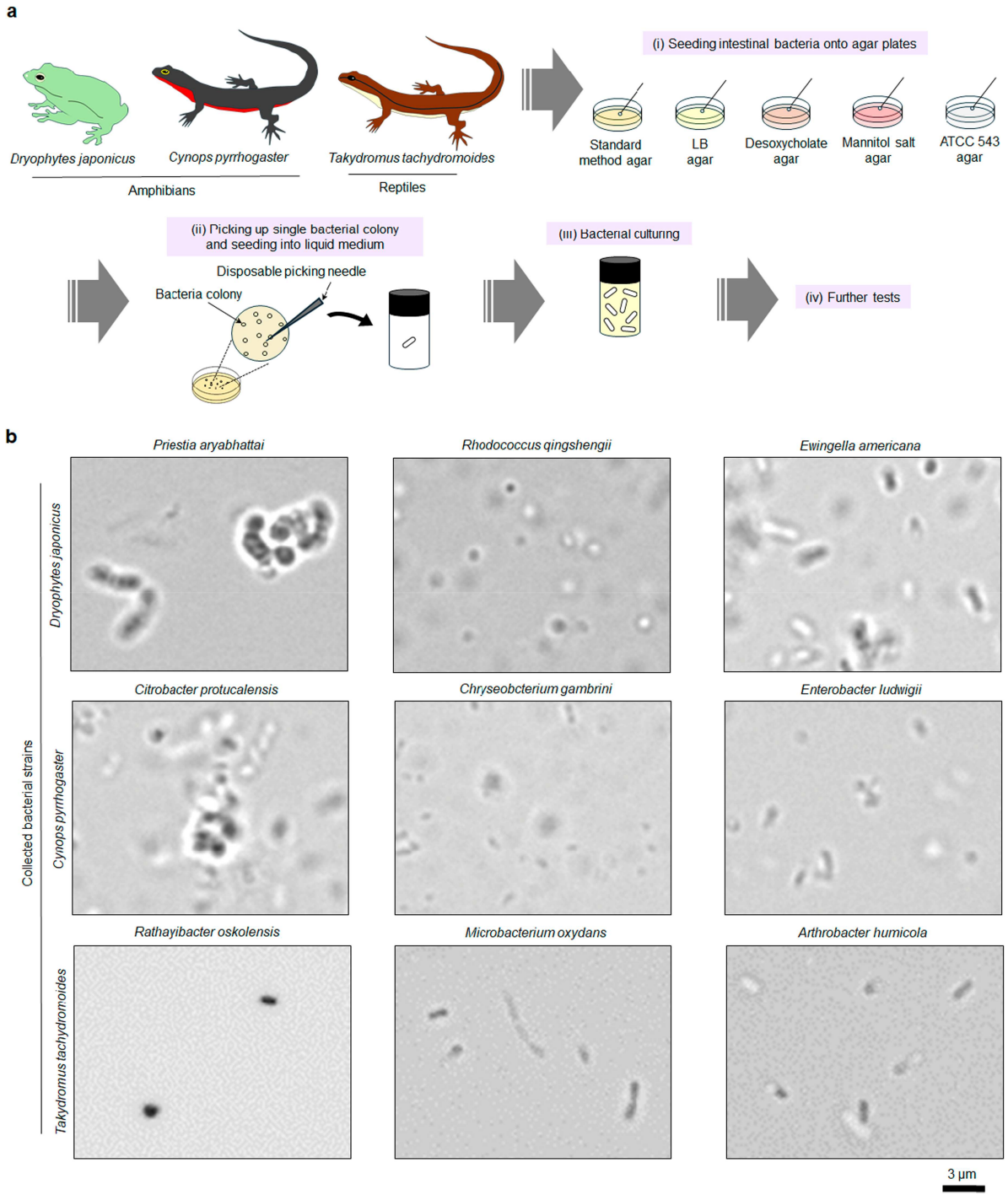

Figure 1. Isolation of gut microbiota from amphibians and reptiles. **(a)** Workflow for isolating gut bacteria from *Dryophytes japonicus*, *Cynops pyrrhogaster* and *Takydromus tachydromoides*. **(b)** Representative optical microscopy images of isolated gut bacterial strains.

successfully obtained and subsequently subjected to preliminary biocompatibility assessment through intravenous administration into BALB/c mice (200 μL via tail vein injection at 5×10^9 CFU/mL) to evaluate acute toxicity and general tolerability profiles (Supplementary Table S1).

Following rigorous biocompatibility screening procedures, nine bacterial strains demonstrating acceptable safety profiles were selected for comprehensive antitumor evaluation: *Priestia aryabhattai* (Bacterial No. 1), *Rhodococcus qingshengii* (Bacterial No. 2), and multiple isolates of *Ewingella americana* (Bacterial No. 3, 6, 7, 9, 10, and 11) obtained from *Dryophytes japonicus*; *Citrobacter portucalensis* (Bacterial No.

16), *Chryseobacterium gambrini* (Bacterial No. 22), and *Enterobacter ludwigii* (Bacterial No. 24) isolated from *Cynops pyrrhogaster*; and *Rathayibacter oskolensis* (Bacterial No. 28, 42), *Microbacterium oxydans* (Bacterial No. 29, 32, and 43), and *Arthrobacter humicola* (Bacterial No. 30) derived from *Takydromus tachydromoides* (Figure 1b). Bacterial species identification was confirmed through 16S rRNA gene sequencing and subsequent Basic Local Alignment Search Tool (BLAST) analyzes to ensure taxonomic accuracy (Supplementary Table S2–S10).

Morphological and growth characteristics revealed distinct phenotypic properties among the isolated strains. On solid agar media, *R. oskolensis* and *M. oxydans* formed characteristic yellow-pigmented colonies, whereas the remaining bacterial strains produced white or cream-colored colonies. Growth optimization studies demonstrated that *E. americana*, *R. oskolensis*, and *M. oxydans* exhibited robust growth across multiple culture media formulations. However, to maximize bacterial yield and viability, LB medium was selected as the optimal growth medium for *R. oskolensis* and *M. oxydans*, while Pearl Core medium provided superior growth conditions for *E. americana*. All nine selected bacterial strains were subsequently propagated in liquid culture medium at room temperature (25 °C) under controlled conditions and maintained for subsequent experimental applications.

In vivo antitumor efficacy of isolated gut bacteria

To systematically evaluate the in vivo antitumor potential of the nine selected gut bacterial isolates, we employed a well-established murine Colon-26 carcinoma syngeneic tumor model that recapitulates key features of human colorectal cancer while maintaining immunocompetence (Figure 2a). This experimental approach enables assessment of both direct bacterial cytotoxicity and host immune-mediated antitumor responses in a physiologically relevant context. When established Colon-26 tumors reached approximately 200 mm^3 in volume, tumor-bearing immunocompetent mice received single intravenous administrations via tail vein injection of 200 μL bacterial suspensions (5×10^9 CFU/mL) or phosphate-buffered saline (PBS) as negative controls. Tumor growth dynamics were monitored longitudinally for 40 days post-treatment to capture both acute and sustained therapeutic responses. We conducted pilot experiments testing a dose range of 2×10^7 to 1×10^9 CFU and found that 1×10^9 CFU provided optimal therapeutic efficacy while maintaining excellent safety profiles (Supplementary Figure S1).

PBS administration served as an appropriate negative control and had no detectable impact on tumor growth kinetics, confirming that the injection procedure itself did not influence tumor progression. Among the bacterial strains isolated from *Dryophytes japonicus*, *P. aryabhattai* demonstrated no measurable antitumor activity compared with PBS-treated controls, indicating that not all gut bacteria possess intrinsic anticancer properties. In contrast, both *R. qingshengii* and *E. americana* achieved significant tumor growth suppression relative to control treatments (Figure 2b and Supplementary Figure S2). Most remarkably, *E. americana* demonstrated exceptional therapeutic efficacy, achieving potent tumor suppression and complete tumor regression (complete response, CR) following a single bacterial administration. The therapeutic kinetics revealed that mice treated with *R. qingshengii* exhibited initial tumor suppression up to day 5 post-injection; however, tumor re-growth was subsequently observed, suggesting that while this strain possesses antitumor activity, its therapeutic effects are not sustained long-term.

Evaluation of bacterial strains isolated from *Cynops pyrrhogaster* revealed that *C. portucalensis*, *C. gambrini*, and *E. ludwigii* all significantly suppressed tumor growth compared with PBS controls (Figure 2c and Supplementary Figure S3). Notably, treatment with *C. portucalensis* and *E. ludwigii* induced complete tumor regression by day 3 post-treatment, demonstrating rapid and potent antitumor efficacy. However, tumor recurrence was observed after day 8 in both treatment groups, indicating that while these strains can achieve initial tumor elimination, they may not provide long-term tumor control. Similarly, administration of bacterial strains isolated from *Takydromus tachydromoides*, including *R. oskolensis*, *M. oxydans*, and *A. humicola*, resulted in significant inhibition of tumor growth relative to control treatments (Figure 2d and Supplementary Figure S4).

Comprehensive analysis of therapeutic outcomes revealed distinct patterns of antitumor activity among the nine gut bacterial isolates. Specifically, one strain (*P. aryabhattai*) exhibited no detectable

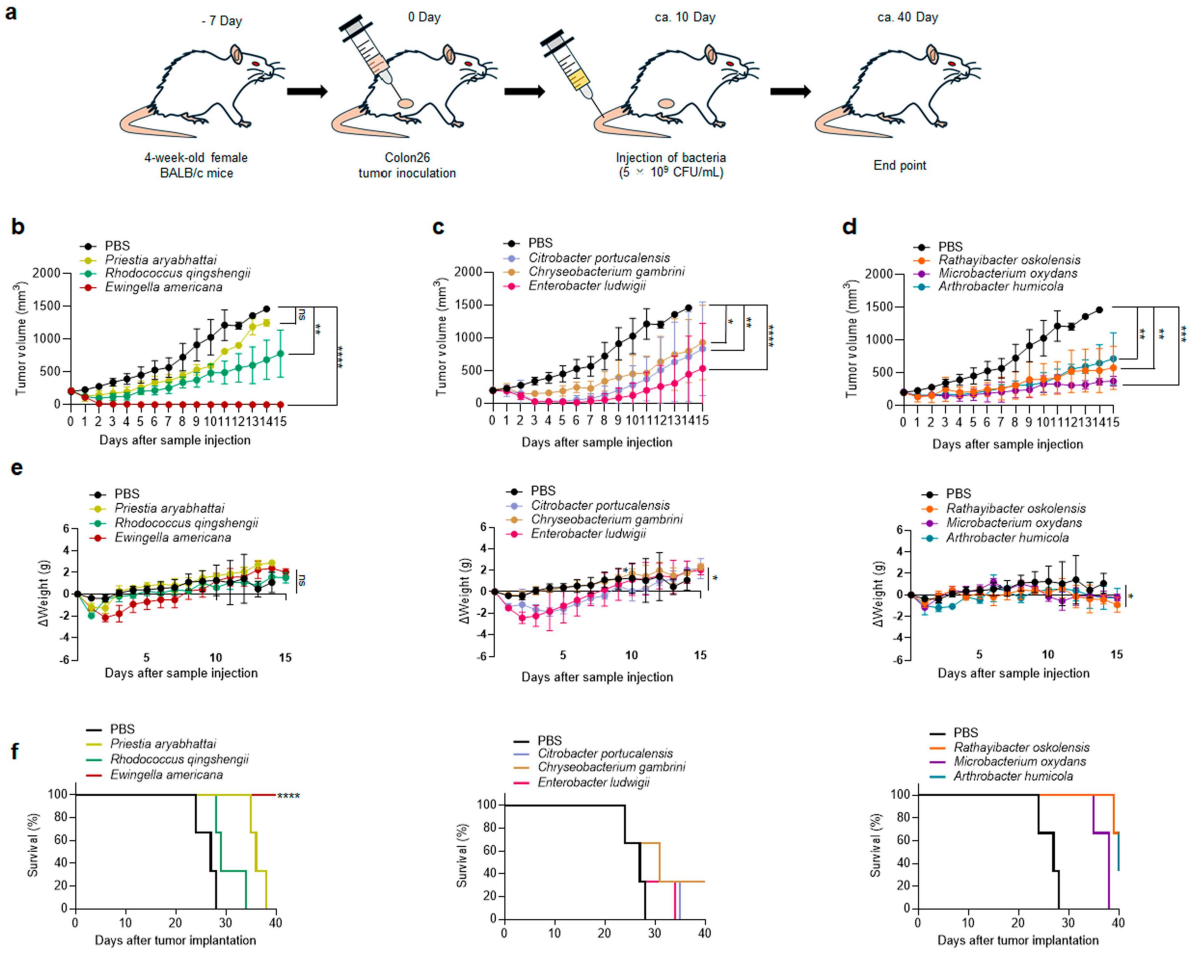

Figure 2. Antitumor activity of gut microbiota in Colon26-bearing BALB/c mice. **(a)** Experimental timeline: tumor inoculation followed by a single intravenous (i.v.) administration of gut bacterial strains. **(b)** Antitumor efficacy of bacteria isolated from *D. japonicus*. Each strain administered via a single tail-vein injection (200 µL, 5×10^9 CFU/mL); PBS served as control. Data shown as mean ± SEM ($n = 3$). Statistical comparison versus PBS: ns, not significant; **, $p < 0.01$; ****, $p < 0.0001$ (Student's two-sided t-test). **(c)** Efficacy of bacteria from *C. pyrrhogaster* (200 µL, 5×10^9 CFU/mL). Data: mean ± SEM ($n = 3$). *, $p < 0.05$; **, $p < 0.01$; ****, $p < 0.0001$ (Student's two-sided t-test). **(d)** Efficacy of bacteria from *T. tachydromoides* (200 µL, 5×10^9 CFU/mL). Data: mean ± SEM ($n = 3$). **, $p < 0.01$; ****, $p < 0.0001$ (Student's two-sided t-test). **(e)** Body-weight monitoring following treatment. Data: mean ± SEM ($n = 3$). ns, not significant; *, $p < 0.05$ (Student's two-sided t-test). Changes in body weight (Δweight, g) were monitored daily throughout the treatment period. All bacterial treatments maintained body weight within acceptable ranges, with no animals experiencing weight loss exceeding 20% of baseline (the predetermined humane endpoint criterion as described in Methods). **(f)** Kaplan–Meier survival curves up to day 40 post–tumor implantation ($n = 3$). ****, $p < 0.0001$ (log-rank [Mantel–Cox] test).

antitumor activity, five strains (*R. qingshengii*, *C. gambrini*, *R. oskolensis*, *M. oxydans*, and *A. humicola*) demonstrated significant tumor growth suppression, and three strains (*E. americana*, *C. portucalensis*, and *E. ludwigii*) achieved both tumor growth suppression and active tumor regression. Importantly, safety monitoring throughout the treatment period revealed that none of the bacterial treatments induced significant body weight loss (Figure 2e), with body weight changes remaining within ±20% of baseline values, indicating the absence of major adverse impacts on host health and physiological homeostasis. Furthermore, *E. americana* administration significantly prolonged overall survival compared with PBS controls, with treated mice achieving 100% survival rates and complete response (CR) rates (Figure 2f).

Tumor rechallenge experiments demonstrated complete tumor rejection in all *E. americana*-cured mice (0/10 developed tumors) versus uniform tumor growth in naïve controls (10/10), providing evidence of durable antitumor immunity with immunological memory persisting beyond 60 days (Supplementary Figure S5). This distinguishes bacterial immunotherapy from conventional treatments that lack memory

generation, suggesting applications as adjuvant therapy preventing recurrence or consolidation therapy after initial tumor reduction.

A particularly intriguing observation emerged from the analysis of bacterial characteristics associated with tumor regression capability. The three bacterial strains that successfully induced tumor regression (*E. americana*, *C. portucalensis*, and *E. ludwigii*) were all identified as facultative anaerobic bacteria. This finding is consistent with established principles of bacterial cancer therapy, as anaerobic bacteria possess the unique capability to selectively accumulate and colonize within solid tumors due to the characteristically hypoxic and immunosuppressive tumor microenvironment.[26,27] This selective tumor colonization likely enabled efficient intratumoral bacterial proliferation and, in conjunction with activated immune cell responses, contributed significantly to the observed tumor regression phenomena.

E. americana, isolated from *Dryophytes japonicus*, is a Gram-negative facultative anaerobic bacterium that belongs to the *Enterobacteriaceae* family. While this species has been occasionally associated with opportunistic infections in neonates and immunocompromised patients in clinical settings, it is generally recognized as having low pathogenic potential, with opportunistic rather than obligate virulence characteristics.[28,29] Additionally, *E. americana* typically exhibits limited antibiotic resistance profiles and remains susceptible to multiple clinically available antimicrobial agents,[28,29] suggesting that potential adverse effects could be effectively managed through targeted antibiotic intervention if required, thereby reducing the likelihood of severe toxicity complications. To our knowledge, this represents the first reported demonstration that a naturally occurring gut bacterium isolated from a wild host organism achieved complete tumor regression following a single intravenous administration. Given its exceptional antitumor efficacy combined with favorable safety characteristics, *E. americana* was selected as the primary candidate for subsequent detailed mechanistic investigations and comprehensive therapeutic evaluation.

Comparative analysis of E. americana anticancer efficacy versus conventional therapeutic agents

To rigorously assess the therapeutic potential of *E. americana* and position its efficacy within the context of established cancer treatments, we conducted comprehensive comparative studies evaluating its anticancer activity against conventional therapeutic agents. Specifically, we compared *E. americana* with the immune checkpoint inhibitor anti-PD-L1 antibody (Anti-PD-L1) and the widely used chemotherapeutic liposome-based nanomedicinal agent doxorubicin (DOX) using the same Colon-26 tumor-bearing mouse model (Figure 3a). The experimental design employed clinically relevant dosing regimens: *E. americana* was administered as a single intravenous injection via tail vein at a dose of 200 μL (5×10^9 CFU/mL), while anti-PD-L1 and DOX were administered intravenously every other day for four total injections at 2.5 mg/kg, representing standard therapeutic protocols.

Comparative efficacy analysis revealed that both anti-PD-L1 and DOX achieved significant tumor growth inhibition compared with PBS-treated controls, confirming the antitumor activity of these established therapies in our experimental model. However, *E. americana* demonstrated markedly superior antitumor effects, substantially outperforming both conventional treatments (Figure 3b, c). While anti–PD-L1 and DOX effectively suppressed tumor progression and delayed tumor growth, only one complete response (CR) was observed in the anti–PD-L1–treated group, and neither therapy achieved consistent tumor eradication across the cohort. In striking contrast, *E. americana* completely eliminated tumor cells and achieved a 100% CR rate across all treated animals (Figure 3d). Furthermore, a single administration of *E. americana* extended mouse survival by at least 30 days compared with PBS-treated controls, demonstrating both superior efficacy and sustained therapeutic benefit (Figure 3e).

The observed superiority of *E. americana* over conventional therapies can be attributed to fundamental differences in their mechanisms of action and tumor-targeting capabilities. PD-L1 is a critical immune checkpoint protein that binds to the PD-1 receptor on T cells, thereby suppressing T cell activity and serving as a primary mechanism through which tumors evade anti-tumor immunity.[30-32] Tumor cells frequently exploit PD-L1 overexpression to escape immune surveillance, facilitating tumor progression and metastasis. Although PD-L1 inhibitors play increasingly important roles in modern cancer immunotherapy, they lack inherent tumor-targeting capability, resulting in systemic distribution and potentially

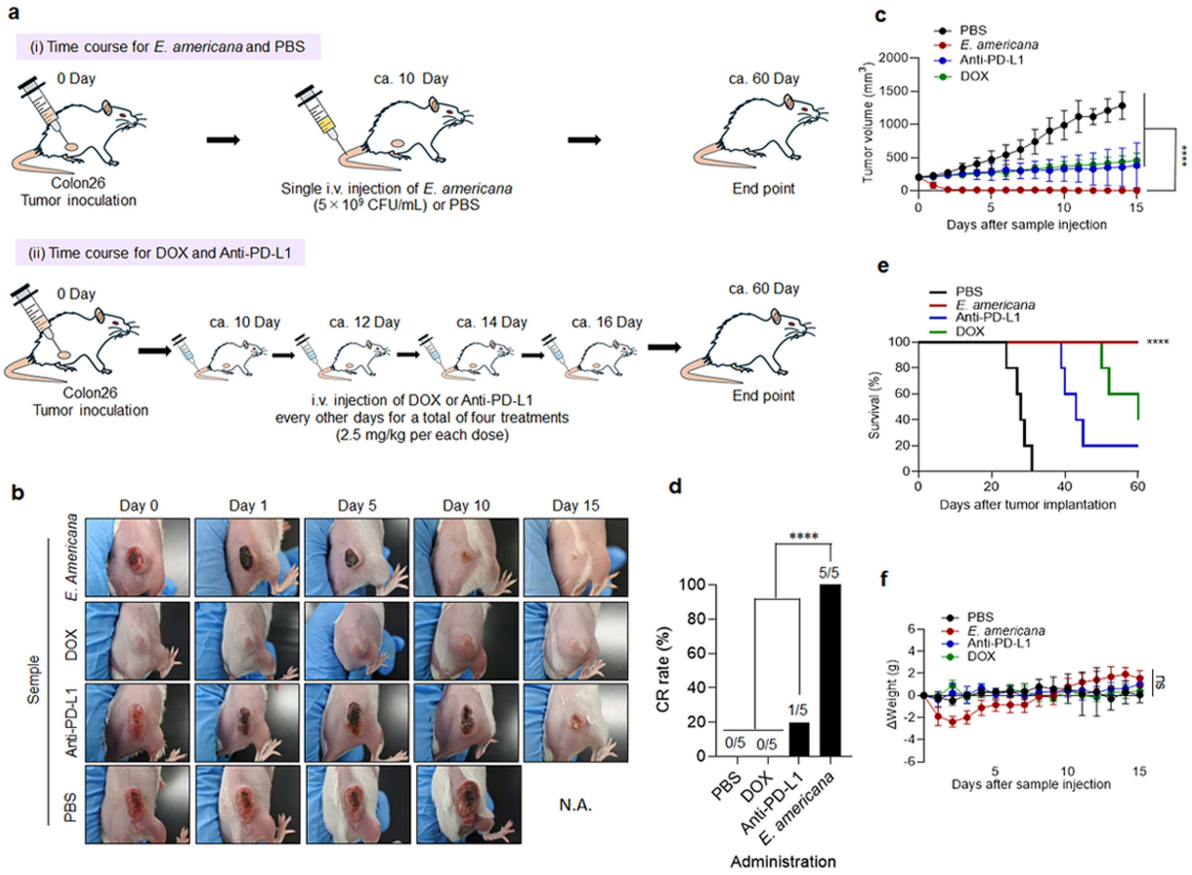

Figure 3. Anticancer efficacy: *Ewingella americana* versus conventional therapies**.** **(a)** Experimental design showing treatment schedules for *E. americana* (single i.v. injection), anti-PD-L1 antibody (four i.v. injections every other day), and doxorubicin (four i.v. injections every other day). All treatment groups in panels (b-f) were evaluated simultaneously using a shared PBS control group to minimize inter-experimental variability and ensure rigorous comparison under identical conditions. **(b)** Representative mouse images post-treatment; N.A., not available. **(c)** Tumor response: single i.v. dose of *E. americana* (200 µL, 5×10^9 CFU/mL); four doses of doxorubicin or anti–PD-L1 (200 µL, 2.5 mg/kg per dose); PBS as control. Data: mean ± SEM ($n = 5$). ****, $p < 0.0001$ (Student's two-sided t-test). **(d)** Complete response rate at day 30 post-treatment. Data: mean ± SEM ($n = 5$). ****, $p < 0.0001$ (Student's two-sided t-test). **(e)** Kaplan–Meier survival curves up to day 60 ($n = 5$). ****, $p < 0.0001$ (log-rank test). **(f)** Body-weight monitoring: single *E. americana* dose, four conventional-drug doses, or single PBS dose. Data: mean ± SEM ($n = 5$). ns, not significant (Student's two-sided t-test).

suboptimal therapeutic efficacy. Furthermore, a significant proportion of cancer patients do not respond to PD-L1 antibody treatments, highlighting the urgent need for more effective therapeutic strategies.[33]

DOX represents a cornerstone of chemotherapeutic intervention with multiple well-characterized mechanisms of action, including DNA intercalation and adduct formation, topoisomerase II (TopII) poisoning, free radical generation and oxidative stress induction, and cellular membrane damage through altered sphingolipid metabolism.[34] In this study, we employed a liposomal doxorubicin formulation, which represents an advanced drug delivery system designed to improve therapeutic efficacy while reducing systemic toxicity. Liposomal encapsulation enables enhanced tumor accumulation through the enhanced permeability and retention (EPR) effect, allowing for preferential drug release within the tumor micro-environment.[35,36] Despite these pharmacokinetic advantages, liposomal DOX still exhibits limitations in terms of tumor-specific targeting compared to naturally tumor-homing bacteria, and its therapeutic efficacy remains dependent on passive accumulation mechanisms rather than active tumor colonization.

In contrast to these conventional approaches, *E. americana*, as a facultative anaerobic bacterium, possesses intrinsic tumor-targeting properties that enable specific accumulation within tumor tissues while avoiding healthy organs. This selective tumor colonization allows *E. americana* to exert potent localized therapeutic effects directly within the tumor microenvironment, explaining why a single bacterial administration was sufficient to achieve dramatic and sustained tumor regression. Safety monitoring revealed

that while a slight reduction in body weight was observed shortly after *E. americana* injection, consistent with mild acute inflammatory responses, no significant differences in body weight were noted among treatment groups by day 15 post-treatment, indicating that the bacterial therapy did not adversely affect overall mouse health or physiological homeostasis (Figure 3f).

Mechanistic investigation of E. americana antitumor activity

Given the exceptional anticancer efficacy demonstrated by *E. americana* in the Colon-26 tumor-bearing mouse model, we conducted comprehensive mechanistic investigations to elucidate the underlying biological processes responsible for its therapeutic activity. Our mechanistic analysis encompassed multiple complementary approaches to characterize both direct bacterial effects and indirect host-mediated responses.

First, to assess the tumor-targeting capability and colonization dynamics of *E. americana*, intratumoral bacterial colony assays were performed to quantify bacterial accumulation and proliferation within tumor tissues (Figure 4a). These investigations revealed that the bacterial load within tumors increased approximately 3000-fold between 3 and 24 hours after intravenous administration, demonstrating highly efficient tumor accumulation and rapid intratumoral proliferation. This dramatic increase in bacterial density within tumor tissues confirms the selective tumor-targeting properties of *E. americana* and suggests that the hypoxic tumor microenvironment provides favorable conditions for bacterial growth and therapeutic activity.

To evaluate the direct cytotoxic effects of *E. americana* against cancer cells, we employed three-dimensional Colon-26 tumor spheroid models that better recapitulate the structural organization and cellular interactions present in solid tumors compared to traditional monolayer cultures. Co-culture experiments involving tumor spheroids with *E. americana* at varying bacterial concentrations (5×10^8, 5×10^7, 5×10^6, 5×10^5, and 5×10^4 CFU) revealed dose-dependent and time-dependent spheroid disruption and cancer cell death. Spheroids treated with the highest bacterial concentration (5×10^8 CFU) were largely destroyed within 24 hours, with the majority of cancer cells eliminated through bacterial-mediated cytotoxicity (Figure 4b, c, and Supplementary Data 1). Notably, even at relatively low bacterial concentrations, *E. americana* retained sufficient cytotoxic potency to achieve significant cancer cell destruction thanks to bacterial secreted cytolysins such as hemolysin and exotoxin (Supplementary Figure S6). These findings were corroborated by *in vitro* cytotoxicity assays using the Cell Counting Kit-8 (CCK-8) methodology applied to murine colorectal cancer cells (Colon-26), which demonstrated effective cancer cell elimination across all tested bacterial concentrations (Supplementary Figure S7).

To characterize intratumoral immune responses following bacterial administration, we conducted comprehensive histopathological and immunohistochemical analyzes of tumor tissue sections (Figure 4d, e). Hematoxylin and eosin (H&E) staining and immunohistochemical (IHC) staining protocols were employed to assess tissue architecture and immune cell infiltration patterns. IHC analysis revealed that tumor tissues from *E. americana*-treated mice exhibited prominent expression of multiple immunological biomarkers, including CD19 (B cell marker), CD3 (T cell marker), and CXCR4 (neutrophil marker). Quantitative analysis demonstrated significant increases in immune cell populations compared with control treatments: B cells ($CD19^+$) increased by 3%, T cells ($CD3^+$) by 5%, and neutrophils ($CXCR4^+$) by 30%. These findings indicate robust recruitment and activation of multiple immune cell populations within the tumor microenvironment following *E. americana* treatment.

The kinetics of immune cell recruitment were further characterized through quantitative PCR (qPCR) analysis, which confirmed that B cells, T cells, and neutrophils were recruited into tumor tissues as early as 6 hours after *E. americana* administration (Figure 4f). This rapid immune cell mobilization suggests that bacterial treatment triggers immediate inflammatory responses that contribute to subsequent antitumor effects. Neutrophils, which represented the most substantially increased immune cell population, possess multiple effector mechanisms including neutrophil extracellular trap (NET) formation, direct phagocytosis of tumor cells, and secretion of pro-inflammatory cytokines and chemokines that can recruit additional immune effector cells.[37]

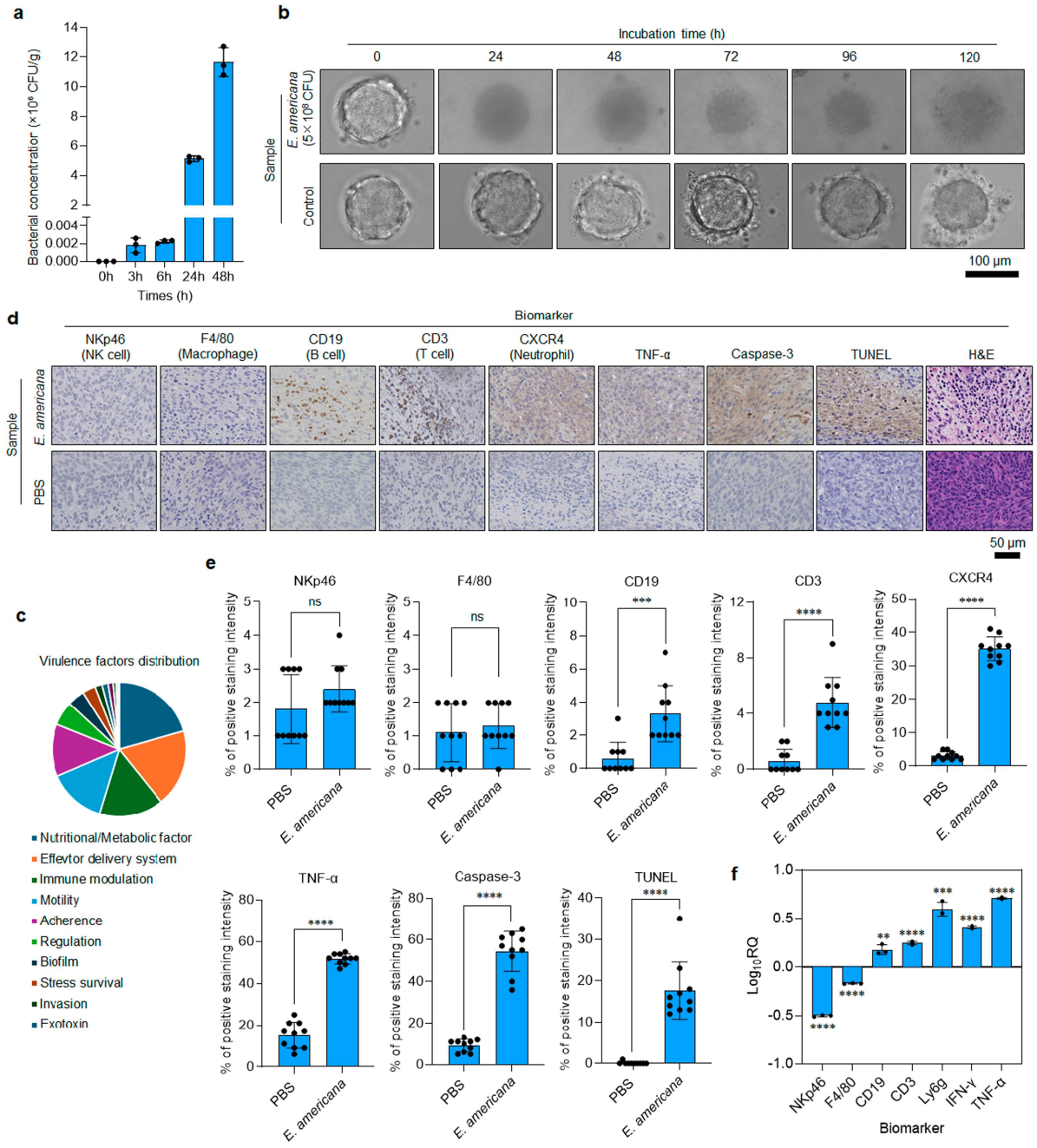

Figure 4. Mechanisms underlying *Ewingella americana* antitumor effects. **(a)** Colony counts in Colon26 tumors following a single i.v. administration of *E. americana* (5×10^9 CFU/mL). Data: mean ± SEM ($n = 3$ experiments). **(b)** Optical microscopy of Colon26 spheroids incubated with or without *E. americana* (5×10^8 CFU). **(c)** Virulence factors distribution of *E. americana*. **(d)** Tumor histology at day 1 post-treatment: H&E, TUNEL, and IHC for NKp46, F4/80, CD19, CD3, CXCR4, TNF-α, caspase-3. **(e)** Quantification of marker-positive cells (10 independent fields per tumor). Data: mean ± SEM. ns, not significant; ***, $p < 0.001$; ****, $p < 0.0001$ (Student's two-sided t-test). **(f)** qPCR (6 h post-i.v.): expression of NKp46, F4/80, CD19, CD3, Ly6G, IFN-γ, TNF-α ($\log_{10}$ fold-change vs untreated control; ACTB as internal control). Data: mean ± SEM ($n = 3$). **, $p < 0.01$; ***, $p < 0.001$; ****, $p < 0.0001$ (Student's two-sided t-test).

Consistent with enhanced immune cell activation, tumor tissues treated with *E. americana* exhibited elevated expression of key inflammatory cytokines, including interferon-γ (IFN-γ) and tumor necrosis factor-α (TNF-α), relative to control treatments. These cytokines play crucial roles in antitumor immunity: IFN-γ enhances antigen presentation and promotes Th1-type immune responses, while TNF-α promotes T cell activation and proliferation,[38] thereby amplifying immune-mediated tumor destruction.

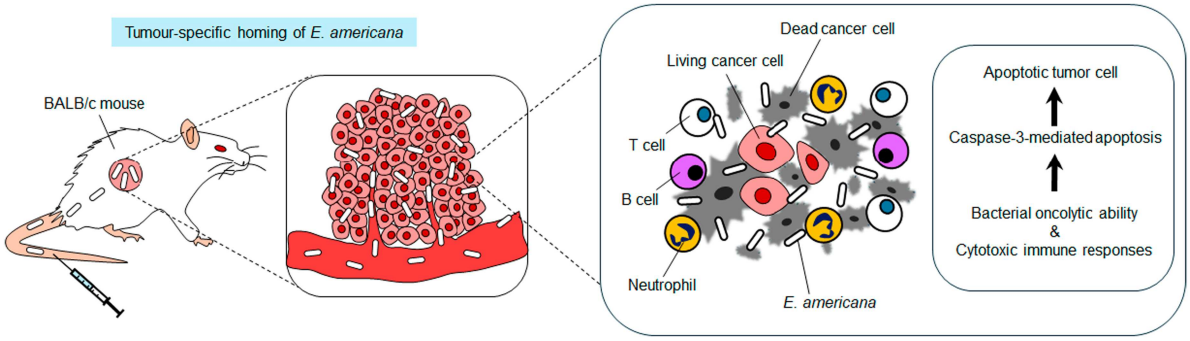

Figure 5. Schematic illustration of the proposed mechanism.

To confirm the induction of tumor cell death, we employed complementary apoptosis detection methodologies, including Caspase-3 immunostaining and terminal deoxynucleotidyl transferase dUTP nick end labeling (TUNEL) assays. Both techniques revealed widespread apoptosis throughout tumor tissues treated with *E. americana*, confirming extensive tumor cell death. Additionally, H&E staining demonstrated significant tissue destruction and architectural disruption in treated tumors compared with fresh tumor tissue obtained from PBS-treated control mice.

Collectively, these mechanistic investigations demonstrate that *E. americana* employs a multifaceted approach to achieve tumor elimination, combining direct bacterial-mediated cytotoxicity with robust activation of host immune responses (Figure 5). The bacterium efficiently infiltrates and proliferates within tumors, where it exerts direct cytotoxic effects while simultaneously activating immune cells (particularly T cells, B cells, and neutrophils) to effectively eliminate cancer cells through complementary mechanisms.

Biocompatibility and safety evaluation of E. americana

Given the critical importance of therapeutic safety in bacterial cancer therapy, we conducted comprehensive evaluations of the systemic effects and biocompatibility of *E. americana* administration. These safety assessments were designed to detect potential adverse effects on major organ systems and physiological parameters that could limit clinical translation.

Hematological and biochemical analyzes were performed 7 days after bacterial administration to assess systemic toxicity. Mouse blood samples were collected for complete blood count (CBC) determinations, including white blood cell count (WBC), platelet count (PLT), hematocrit (HCT), hemoglobin concentration (HGB), mean corpuscular hemoglobin (MCH), mean corpuscular hemoglobin concentration (MCHC), mean corpuscular volume (MCV), and red blood cell count (RBC). Additionally, plasma samples were analyzed for comprehensive biochemical parameters to evaluate liver function, kidney function, and metabolic status (Figure 6a and Supplementary Table S11).

Comprehensive analysis of hematological and biochemical parameters revealed no significant differences between *E. americana*-treated mice and PBS-treated control groups across all measured parameters. These findings indicate that bacterial treatment did not induce detectable hematological toxicity, hepatotoxicity, nephrotoxicity, or metabolic dysfunction, suggesting excellent systemic biocompatibility.

To evaluate potential organ-specific toxicity, major organs including liver, spleen, heart, lungs, and kidneys were harvested 30 days post-treatment and subjected to detailed histopathological analysis using hematoxylin and eosin (H&E) staining protocols (Figure 6b). Microscopic examination of tissue sections revealed no evidence of bacterial existence, tissue damage, inflammatory infiltration, necrosis, or other pathological alterations attributable to bacterial administration in any examined organ. These histological findings confirm that *E. americana* treatment does not cause detectable organ toxicity or structural damage to vital organs.

We have performed acute toxicity studies with blood collection at multiple early timepoints (24 hours, 48 hours, 72 hours, and 240 hours post-injection) (Supplementary Table S14–S17). These analyzes confirm

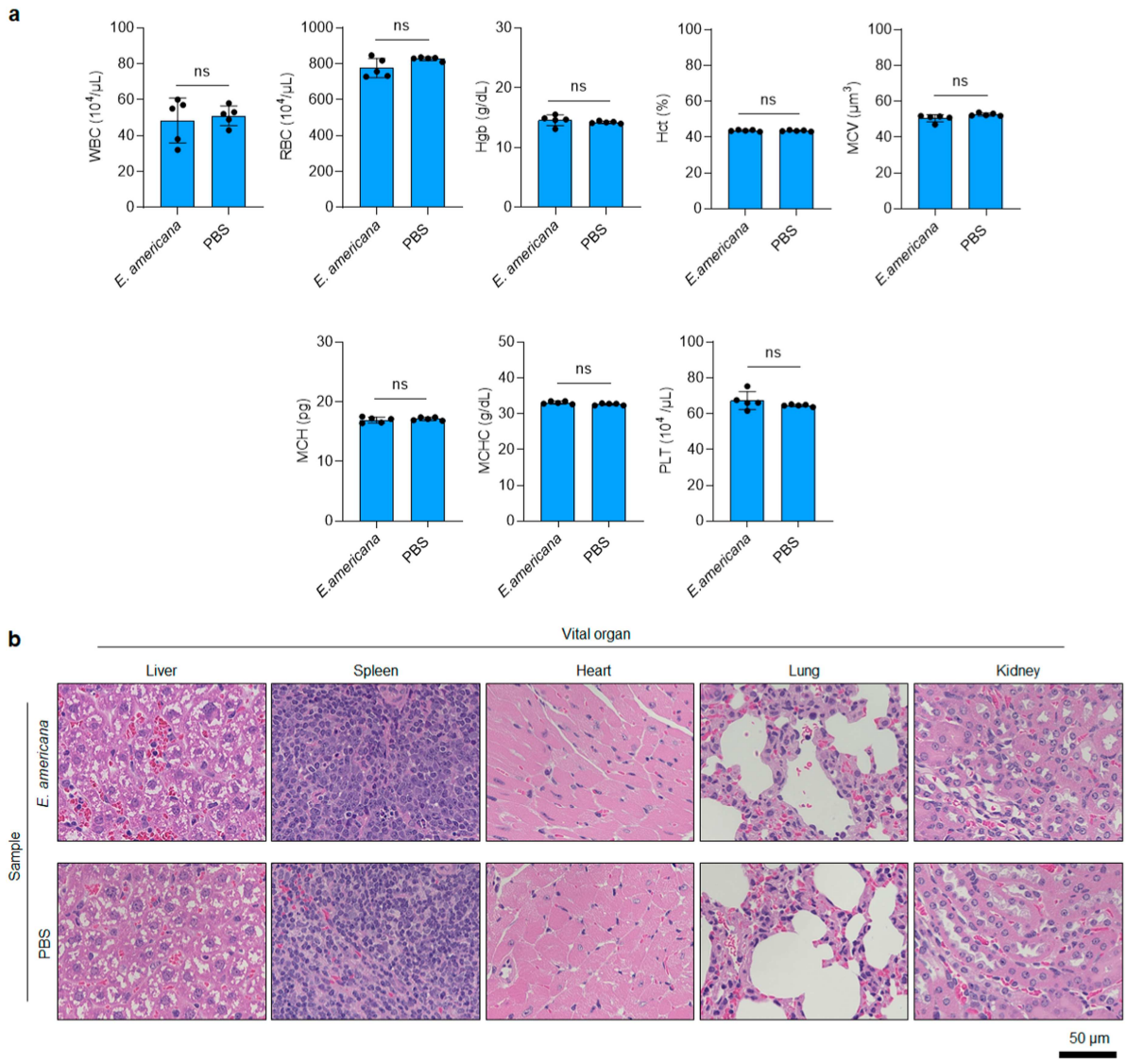

Figure 6. Biocompatibility of *Ewingella americana*. **(a)** Complete blood counts at day 30 (5×10^9 CFU/mL *E. americana* or PBS). Data: mean ± SEM ($n = 5$). Definitions: WBC, white blood cells; RBC, red blood cells; HGB, hemoglobin; HCT, hematocrit; MCV, mean corpuscular volume; MCH, mean corpuscular hemoglobin; MCHC, mean corpuscular hemoglobin concentration; PLT, platelets. ns, not significant (Student's two-sided t-test). All values within normal physiological ranges for BALB/c mice (manufacturer's data). **(b)** Histopathology (H&E) of major organs at day 30 post-treatment with *E. americana* or PBS.

that *E. americana* administration induces only transient, mild responses that resolve within 240 hours. Extended observation (60 days) confirmed sustained safety without chronic toxicity. As a naturally occurring, antibiotic-susceptible strain,[28] *E. americana* offers advantages over genetically engineered bacteria regarding regulatory pathways and safety intervention capabilities.

Blood bacterial colony assays performed at 0.08 (5 min), 3, 24, and 48 hours post-injection demonstrated rapid clearance kinetics, with bacteria becoming completely undetectable by 24 hours (Supplementary Figure S8). This rapid systemic clearance, coupled with tumor-exclusive colonization, explains the favorable safety profile. These results suggest that *E. americana* is effectively cleared by immune cells following tumor eradication and does not exert adverse effects on host physiology.

The excellent safety profile observed in our studies can be attributed to several factors. First, the naturally occurring, non-pathogenic characteristics of the gut-derived *E. americana* strain likely contribute to its biocompatibility. Second, the apparent effective clearance of bacteria by host immune cells

following tumor eradication prevents bacterial persistence and potential long-term complications. These results suggest that *E. americana* represents a promising therapeutic candidate with an acceptable safety profile suitable for potential clinical development.

Discussion

In this comprehensive study, we have demonstrated that bacterial strains isolated from the intestinal microbiomes of amphibians and reptiles exhibit remarkable anticancer activity with significant therapeutic potential. Among the nine bacterial strains systematically evaluated, eight displayed significant antitumor effects following single intravenous administrations, highlighting the therapeutic richness of these unexplored microbial communities. Most notably, *E. americana*, isolated from the Japanese tree frog *Dryophytes japonicus*, achieved exceptional therapeutic outcomes including complete tumor remission (CR) due to its robust and sustained anticancer efficacy.

Our mechanistic investigations have elucidated that *E. americana* employs a sophisticated dual-action therapeutic mechanism involving both direct and indirect antitumor effects. The underlying therapeutic mechanism encompasses selective tumor colonization and proliferation by this facultative anaerobic bacterium, coupled with potent direct cytotoxic effects against cancer cells and comprehensive immune-mediated tumor suppression through coordinated activation of neutrophils, T cells, and B cells. The recruited immune cell populations release pro-inflammatory cytokines, particularly TNF-α and IFN-γ, which further amplify immune activation and induce substantial apoptosis throughout tumor tissues. Importantly, *E. americana*, being isolated from a natural host organism, demonstrated exceptional biocompatibility with no evidence of systemic toxicity or adverse effects on major organ systems, thereby establishing its promise in terms of both efficacy and safety.

Our subcutaneous Colon-26 model, while differing from orthotopic colorectal cancer models, provides critical advantages for proof-of-concept bacterial therapy studies. This model enables unambiguous demonstration of tumor-specific homing through bloodstream circulation, independent of anatomical proximity to the gastrointestinal tract. Importantly, our findings have direct clinical relevance to metastatic disease, where tumors are anatomically distant from gut microbiota (liver, lung, peritoneum). The syngeneic immunocompetent model preserves essential host-bacterial-tumor immune interactions, crucial for evaluating immunomodulatory mechanisms. Future orthotopic studies will provide complementary insights into bacterial-gut microbiota interactions.

E. americana's exceptional tumor specificity likely arises from multiple synergistic mechanisms beyond hypoxia alone. Tumor cells overexpress CD47 ("don't eat me" signal),[39,40] creating locally immunosuppressed microenvironments permitting bacterial persistence, while intact immune surveillance in healthy organs rapidly clears bacteria. Additional tumor-specific features—necrotic regions, aberrant vasculature facilitating bacterial extravasation,[41] altered metabolic byproducts, and disrupted extracellular matrix—synergistically support selective colonization. Our colony assays and histopathological analyzes demonstrate bacterial recovery exclusively from tumors, with zero detectable colonization in lung, liver, spleen, kidney, or heart. Since physiological hypoxia exists in certain normal tissues (intestinal crypts, renal medulla), the complete absence of bacterial colonization in these sites confirms that hypoxia is necessary but insufficient, and the unique tumor microenvironment constellation creates a permissive niche for *E. americana*.

E. americana achieved superior outcomes (100% CR) versus anti-PD-L1 (tumor suppression only), reflecting fundamentally different immune activation mechanisms. Anti-PD-L1 passively removes inhibitory signals on pre-existing T cells ("releasing brakes"), whereas *E. americana* actively stimulates immunity through PAMPs (pathogen-associated molecular patterns), triggering robust innate immune activation through pattern recognition receptors including Toll-like receptors (TLRs) and NOD-like receptors (NLRs)[42] that recruits neutrophils, macrophages, and NK cells while initiating de novo inflammatory cascades. This mechanistic orthogonality is evidenced by distinct immune infiltration patterns—*E. americana* induced dramatic neutrophil recruitment[43] that directly contributes to tumor destruction, while checkpoint inhibitors minimally affect neutrophil populations. These differences suggest potential synergy in combination therapy and indicate bacterial therapy may benefit checkpoint inhibitor-resistant

patients, particularly those with "cold" tumors lacking T cell infiltration,[44] which represent a significant proportion of patients who fail conventional immunotherapy.

Our comparator selection was strategic: anti-PD-L1 represents best-in-class immunotherapy with broad clinical adoption, enabling assessment of bacterial therapy advantages over current immunotherapy standards. Liposomal doxorubicin (FDA-approved nanoformulation) represents state-of-the-art drug delivery technology; demonstrating superiority establishes that biological tumor targeting outperforms sophisticated pharmaceutical delivery systems. These comparators facilitate mechanistic insights (immune-based vs. cytotoxic) and literature comparison. Future studies will include colorectal-specific regimens (5-FU, FOLFOX) for comprehensive benchmarking.

Pharmacokinetic studies revealed favorable kinetics: rapid blood clearance coupled with efficient tumor accumulation. This profile explains both excellent safety and potent efficacy with single-dose administration. Biodistribution analyzes confirmed tumor-exclusive localization. These characteristics compare favorably with chemotherapy agents exhibiting prolonged systemic exposure and normal tissue accumulation. Peak intratumoral bacterial burden (48 hours) provides rational timing for combination therapies.

The therapeutic mechanism—hypoxia-driven colonization and PAMP-mediated immune activation—relies on features common to most solid tumors, suggesting broad applicability. Literature supports this: tumor-targeting bacteria demonstrate efficacy across various cancer models.[15,17,20] Hypoxic, immunologically "cold" tumors (pancreatic cancer, triple-negative breast cancer) may be particularly responsive. Our spheroid experiments demonstrate direct cytotoxicity operating through universal cellular targets. Future studies in other cancer models will definitively establish broad-spectrum activity.

Our dose-finding studies identified 1×10^9 CFU as both the optimal therapeutic dose and maximum tolerated dose, indicating a narrow therapeutic window that requires careful consideration for clinical translation. However, comprehensive safety evaluation at this dose revealed only transient, self-limiting inflammatory responses with complete resolution by 72 hours and no organ toxicity. Pharmacokinetic analysis demonstrated rapid bacterial clearance from blood (undetectable by 24 hours) with selective tumor accumulation, explaining the acceptable safety profile despite narrow margins. For clinical development, several strategies can optimize the therapeutic index: dose fractionation to avoid peak systemic burden, intratumoral injection for accessible tumors, combination with lower bacterial doses plus checkpoint inhibitors, and intensive monitoring with antibiotic intervention capability as a fail-safe mechanism. Species differences in immune responses and allometric scaling with appropriate safety factors will guide safe starting doses for human trials.

For clinical translation, key considerations include: GMP manufacturing protocols ensuring batch consistency;[45] patient selection focusing on advanced solid tumors with documented hypoxia; dose-escalation trials with intensive safety monitoring; and exploration of combination strategies with checkpoint inhibitors (potentially synergistic), chemotherapy (enhanced drug delivery), and radiation (tumor sensitization). Investigation of multiple dosing schedules, intratumoral injection for accessible tumors, and autologous microbiome screening represent promising avenues for personalized bacterial therapy.

Future investigations should explore alternative administration routes, particularly oral delivery, which could offer advantages in patient convenience and accessibility. However, oral administration of *E. americana* would require development of protective formulation strategies (enteric coating, acid-resistant capsules) to ensure bacterial survival through gastric acid and successful translocation from gut to tumor sites. Such formulation-based approaches would be especially relevant for treating primary colorectal tumors or liver metastases where anatomical proximity facilitates bacterial translocation. While technically challenging, oral delivery strategies could expand clinical applicability and enable investigation of administered bacteria-host microbiota interactions, representing a promising direction for future research beyond the intravenous approach validated in the current study.

Current cancer therapeutic approaches leveraging gut microbiota have primarily focused on microbiome modulation strategies or fecal microbiota transplantation protocols rather than direct bacterial administration. However, the intestinal tract represents a vast repository of bacterial diversity, harboring numerous species that remain insufficiently characterized despite possessing unique metabolic pathways, bioactive compound production capabilities, and immunomodulatory properties with potential therapeutic applications. The present study highlights the tremendous potential of systematically exploring and harnessing these underexplored microbial resources for innovative antitumor therapy approaches.

Our findings underscore the critical need for expanded research efforts focused on comprehensive bacterial strain characterization, detailed mechanistic investigations of bacterial-host interactions, and the systematic development of novel therapeutic strategies toward clinical application. The exploration of diverse bacterial communities from phylogenetically distinct host species may yield additional therapeutic candidates with complementary or enhanced anticancer properties. Furthermore, the development of optimized bacterial delivery systems, combination therapeutic approaches, and personalized treatment protocols based on individual patient microbiome profiles represents promising avenues for future investigation.

The successful identification of *E. americana* as a potent, naturally occurring anticancer agent establishes a proof-of-concept for microbiome-derived bacterial therapeutics and provides a foundation for the development of a new class of cancer treatments. These discoveries may ultimately lead to transformative advances in precision oncology and offer new hope for patients with treatment-refractory cancers. Future research directions should focus on expanding bacterial discovery programs, optimizing therapeutic protocols, investigating combination therapies, and advancing promising candidates toward clinical translation to fully realize the therapeutic potential of microbiome-derived cancer therapeutics.

This study provides novel insights into the therapeutic potential of previously uncharacterized gut microbes from lower vertebrates and establishes a foundation for the development of naturally occurring bacterial therapeutics in cancer treatment. Our findings demonstrate the vast untapped potential residing within diverse microbial ecosystems and highlight the critical importance of biodiversity conservation efforts in advancing medical science and therapeutic innovation.

Methods

Experimental animals and ethical approval

All animal experiments were conducted in strict accordance with protocols approved by the Institutional Animal Care and Use Committee of the Japan Advanced Institute of Science and Technology (Approval No. 07-001) and performed according to the Guidelines for Animal Experimentation established by the Japanese Association of Laboratory Animal Science. Female BALB/c mice (BALB/cCrSlc strain) aged 5 weeks and weighing 18-21 g were obtained from Japan SLC (Shizuoka, Japan). Animals were maintained in a pathogen-free environment under controlled conditions with a 12-hour light/dark cycle, temperature maintained at 22 ± 2 °C, humidity at 55 ± 10%, and provided ad libitum access to standard laboratory chow and sterile water. Mice were acclimatized for a minimum of 7 days prior to experimental procedures to minimize stress-induced physiological variations.

Collection and isolation of gut microbiota from amphibians and reptiles

Field sampling was conducted with appropriate environmental permits from designated locations in Japan. *Dryophytes japonicus* (Japanese tree frog) and *Takydromus tachydromoides* (Japanese grass lizard) specimens were collected from natural habitats in Ishikawa Prefecture, Japan, while *Cynops pyrrhogaster* (Japanese fire belly newt) specimens were obtained from Okayama Prefecture, Japan. All animal collection procedures were performed in accordance with local wildlife protection regulations and institutional guidelines for field research.

For bacterial isolation, animals were humanely euthanized using appropriate methods to minimize distress, and intestinal sampling was immediately performed under sterile conditions. A sterile inoculation loop was carefully inserted into the intestinal tract of each specimen to collect bacteria adhering to the intestinal surface. The collected material was suspended in sterile phosphate-buffered saline (PBS, pH 7.4) to create bacterial suspensions. Subsequently, 100 μL aliquots of these suspensions were inoculated onto five distinct selective and differential agar media to maximize bacterial recovery and diversity: (1) deoxycholate agar containing sodium deoxycholate, iron ammonium citrate, sodium chloride, dipotassium phosphate, lactose, peptone, and neutral red (Nissui Pharmaceutical Co., Ltd., Tokyo, Japan); (2) mannitol salt agar containing mannitol, sodium chloride, phenol red, meat extract, and peptone (Nissui

Pharmaceutical Co., Ltd.); (3) standard method agar containing yeast extract, peptone, and glucose (Nissui Pharmaceutical Co., Ltd.); (4) Luria-Bertani (LB) agar containing tryptone, sodium chloride, and yeast extract (Nacalai Tesque, Kyoto, Japan); and (5) ATCC 543 agar containing sodium succinate (Nacalai Tesque), Dipotassium hydrogen phosphate (Nacalai Tesque), Potassium dihydrogen phosphate (Nacalai Tesque), Magnesium sulfate heptahydrate (Nacalai Tesque), Ammonium sulfate (Nacalai Tesque), Calcium chloride (FUJIFILM Wako Pure Chemical Corporation, Osaka, Japan), Ferric Ammonium citrate (FUJIFILM Wako Pure Chemical Corporation), EDTA (Dojindo, Kumamoto, Japan), Yeast extract (Becton, Dickinson and Company, Franklin Lakes, NJ, US) and agar powder (FUJIFILM Wako Pure Chemical Corporation).

Inoculated plates were incubated anaerobically for 3 days at room temperature (25 °C) under tungsten lamp illumination to promote bacterial growth while maintaining physiologically relevant conditions. Individual bacterial colonies exhibiting distinct morphological characteristics were carefully isolated using sterile syringe needles under stereomicroscopic guidance to ensure colony purity. Selected colonies were subjected to multiple rounds of streaking and sub-culturing to obtain pure bacterial isolates. A total of 45 distinct bacterial strains were successfully isolated through this systematic approach. Virulence factors of *E. americana* were identified by analyzing the publicly available genome of the type strain ATCC 33852 (NCBI RefSeq: GCF_000735345.1) with the Type Strain Genome Database,[46] rather than by sequencing the isolate obtained in this study.

Bacterial identification and characterization

Bacterial species identification was performed through 16S ribosomal RNA gene sequencing analysis conducted by BEX Co., Ltd. (Tokyo, Japan) using established molecular phylogenetic methods. Briefly, genomic DNA was extracted from pure bacterial cultures, and the 16S rRNA gene was amplified using universal bacterial primers. PCR products were sequenced using Sanger sequencing methodology, and the resulting sequences were compared against the NCBI GenBank database using Basic Local Alignment Search Tool (BLAST) analysis to achieve species-level identification. Through this comprehensive analysis, nine bacterial strains representing distinct species were identified and selected for further investigation: *Priestia aryabhattai*, *Rhodococcus qingshengii*, *Ewingella americana*, *Citrobacter portucalensis*, *Chryseobacterium gambrini*, *Enterobacter ludwigii*, *Rathayibacter oskolensis*, *Microbacterium oxydans*, and *Arthrobacter humicola*.

Bacterial cultivation and growth optimization

Bacterial cultivation protocols were optimized for each strain to achieve maximal growth and viability. All bacterial strains were initially tested on four different agar media to determine optimal growth conditions: deoxycholate agar, mannitol salt agar, standard method agar, and LB agar (all obtained from Nissui Pharmaceutical Co., Ltd. and Nacalai Tesque). Based on growth performance assessments, strain-specific culture conditions were established.

E. americana, *C. gambrini*, and *E. ludwigii* demonstrated optimal growth characteristics in Pearl Core E-MC64 medium (Eiken Chemical Co., Ltd., Tokyo, Japan), which provided superior bacterial yield and viability compared to alternative media. These strains were cultured in Pearl Core medium at room temperature (25 °C) for 5-10 days with regular monitoring to achieve optimal bacterial density. The remaining bacterial strains (*P. aryabhattai*, *R. qingshengii*, *C. portucalensis*, *R. oskolensis*, *M. oxydans*, and *A. humicola*) exhibited superior growth in Luria-Bertani (LB) broth (Nacalai Tesque) and were maintained under identical temperature and time conditions.

For in vivo administration, bacteria were used directly in their respective culture media rather than being resuspended in PBS to maintain optimal bacterial viability and metabolic activity. Specifically, *E. americana*, *C. gambrini*, and *E. ludwigii* were administered in Pearl Core E-MC64 medium, while *P. aryabhattai*, *R. qingshengii*, *C. portucalensis*, *R. oskolensis*, *M. oxydans*, and *A. humicola* were administered in LB broth. This approach preserves bacterial fitness by avoiding osmotic stress that can occur during resuspension in PBS.

Bacterial viability and concentration were confirmed immediately prior to each administration through the following procedures: (1) cell number measurement using a bacterial counter (CASY Cell Counter & Analyzer; OMNI Life Science, Basel, Switzerland); (2) optical density measurements at 600 nm (OD600) to estimate bacterial concentration; (3) serial dilution and colony-forming unit (CFU) counting on agar plates to determine viable bacterial count; and (4) microscopic examination to confirm bacterial morphology and absence of contamination. Bacterial suspensions were prepared fresh for each experiment and used within 2 hours of preparation. Viability assessments consistently demonstrated >95% bacterial viability at the time of administration, with bacterial concentrations maintained at 5×10^9 CFU/mL (±10%) across all experiments to ensure reproducibility.

All bacterial cultures were grown in liquid medium with gentle agitation to ensure adequate oxygenation and nutrient distribution. Bacterial growth was monitored through optical density measurements and colony-forming unit (CFU) determinations to achieve consistent bacterial concentrations for experimental applications. All reagents for bacterial cultivation were obtained from certified suppliers (Nacalai Tesque, Kyoto, Japan; FUJIFILM Wako Pure Chemical Corporation, Osaka, Japan) to ensure reproducibility and quality control.

Preliminary biocompatibility screening

Prior to comprehensive antitumor evaluation, all 45 isolated bacterial strains underwent systematic biocompatibility screening to identify strains with acceptable safety profiles for in vivo administration. Female BALB/c mice (7 weeks old, average weight 20 g, $n = 3$ per group) were intravenously injected via tail vein with 200 μL of culture medium containing individual bacterial strains at standardized concentrations of 5×10^9 CFU/mL.

Biocompatibility assessment criteria included: (1) animal survival for a minimum of 7 days post-injection, (2) body weight maintenance with less than 20% weight loss, (3) absence of severe clinical signs including lethargy, respiratory distress, or neurological symptoms, and (4) normal behavioral patterns and feeding activity. Mice were monitored continuously for the first 24 hours post-injection and subsequently assessed daily for 7 days. Body weight measurements were recorded daily to quantify potential systemic toxicity effects.

Based on these comprehensive safety evaluations, nine bacterial strains demonstrating acceptable biocompatibility profiles were selected for subsequent detailed antitumor efficacy studies. This rigorous screening approach ensured that only bacterial strains with favorable safety characteristics advanced to therapeutic evaluation phases.

Cell culture and maintenance

Murine colon carcinoma (Colon-26) cells were obtained from the Japanese Collection of Research Bioresources Cell Bank (JCRB Cell Bank, Tokyo, Japan) and maintained according to established protocols to ensure cell line authenticity and experimental reproducibility. Colon-26 cells were cultured in Roswell Park Memorial Institute (RPMI) 1640 medium (Gibco, Grand Island, NY, USA) supplemented with 10% fetal bovine serum (FBS), 2 mM L-glutamine, 1 mM sodium pyruvate, and antibiotics including gentamicin and penicillin-streptomycin (100 IU/mL each) to prevent bacterial contamination while maintaining optimal cell growth conditions.

Cells were maintained in a humidified incubator at 37 °C with 5% CO_2 atmosphere to replicate physiological conditions. To avoid genetic instabilities associated with excessive passage numbers, cells were regularly revived from early passage cryopreserved stocks stored in liquid nitrogen. Cell viability and morphology were routinely assessed using trypan blue exclusion assays and microscopic examination to ensure culture quality and experimental consistency.

Therapeutic agent preparation

Conventional therapeutic agents were prepared according to clinical protocols to enable meaningful comparative studies. Liposomal doxorubicin (DOX), an advanced nanoformulation of the widely used

anthracycline chemotherapeutic agent, was obtained as a clinical formulation (2 mg/mL, Baxter K.K., Tokyo, Japan) and stored at 4 °C to maintain stability and preserve liposomal integrity. Anti-PD-L1 antibody, an immune checkpoint inhibitor representative of modern immunotherapy approaches, was obtained from Leinco Technologies (St. Louis, MO, USA) at a concentration of 6 mg/mL and stored at −80 °C to preserve biological activity. Prior to administration, both agents were diluted in sterile saline to achieve desired dosing concentrations according to established protocols, with particular care taken to maintain the structural integrity of the liposomal DOX formulation during dilution procedures.

Dose optimization studies

To determine the optimal bacterial dose for therapeutic efficacy and safety, preliminary dose-finding studies were conducted using *E. americana*. Female BALB/c mice bearing Colon-26 tumors (approximately 200 mm^3, $n = 5$ per dose group) received single intravenous injections of *E. americana* at varying concentrations: 2×10^7, 2×10^8, and 1×10^9 CFU in 200 μL volume. Tumor growth, survival, and body weight were monitored for 8 days post-treatment. Based on these studies, 1×10^9 CFU (5×10^9 CFU/mL) was identified as the optimal dose achieving maximal therapeutic efficacy (complete tumor regression) while maintaining acceptable safety profiles. Doses exceeding 1×10^9 CFU resulted in acute mortality, establishing this as the maximum tolerated dose for subsequent experiments.

In vivo antitumor efficacy evaluation

Comprehensive antitumor efficacy studies were conducted using a well-established syngeneic Colon-26 tumor model that maintains immunocompetence while recapitulating key features of human colorectal cancer. Female BALB/c mice (6 weeks old, average weight 20 g, $n = 5$ per treatment group) were subcutaneously inoculated with 1×10^6 Colon-26 cells suspended in 100 μL of fresh RPMI1640 in the right flank region. Tumor establishment was monitored daily through palpation and caliper measurements.

When tumors reached approximately 200 mm^3 in volume (typically 7-10 days post-inoculation), mice were randomly assigned to treatment groups to minimize selection bias. Bacterial treatments were administered as single intravenous injections via tail vein using 200 μL of culture medium containing each bacterial strain at 5×10^9 CFU/mL. Control groups received equivalent volumes of sterile PBS. Treatment administration was performed under sterile conditions using 29-gauge needles to minimize tissue trauma and ensure accurate delivery.

Tumor growth monitoring was performed daily using digital calipers, and tumor volumes were calculated using the standard ellipsoid formula: $V = L \times W^2/2$, where L represents the longest diameter and W represents the perpendicular width. Body weight measurements were recorded daily to assess potential systemic toxicity. General health status was evaluated through assessment of behavioral patterns, feeding activity, and clinical signs.

Survival analysis was conducted over a 60-day observation period, with humane endpoints established according to institutional guidelines. Mice were euthanized when tumor volumes exceeded 1,500 mm^3, when body weight loss exceeded 20%, or when signs of severe distress were observed, in accordance with approved animal welfare protocols.

To evaluate the induction of long-term antitumor immunity, tumor-free mice that had achieved complete regression following *E. americana* treatment were rechallenged on day 30 post-treatment by subcutaneous injection of 1×10^6 Colon-26 cells into the contralateral flank. Age-matched BALB/c mice were used as controls. Tumor growth was monitored for an additional 30 days.

Comparative therapeutic efficacy studies

To evaluate the therapeutic potential of *E. americana* relative to established cancer treatments, comparative efficacy studies were conducted using identical experimental conditions. Female BALB/c mice bearing

Colon-26 tumors (approximately 200 mm^3) were treated with either a single intravenous injection of *E. americana* (200 μL, 5×10^9 CFU/mL) or conventional therapies administered according to standard clinical protocols.

Conventional therapy groups received either doxorubicin (2.5 mg/kg body weight) or anti-PD-L1 antibody (2.5 mg/kg body weight) administered intravenously every other day for four total doses, representing clinically relevant dosing regimens. All treatments were diluted in sterile saline to achieve appropriate concentrations and administered via tail vein injection under sterile conditions.

Therapeutic responses were assessed through tumor volume measurements, survival analysis, and complete response (CR) rate determinations. Complete response was defined as the absence of palpable tumor mass maintained for a minimum of 30 days following treatment initiation. Partial response, stable disease, and progressive disease categories were defined according to established preclinical oncology criteria. All treatment groups were evaluated simultaneously using a shared PBS control group to minimize inter-experimental variability and ensure rigorous comparison under identical conditions.

Intratumoral bacterial colonization assessment

To investigate the tumor-targeting capabilities of *E. americana*, quantitative bacterial colony assays were performed to assess intratumoral bacterial accumulation and proliferation dynamics. Female BALB/c mice bearing Colon-26 tumors (approximately 200 mm^3) received intravenous injections of *E. americana* (200 μL, 5×10^9 CFU/mL). At predetermined time points (3, 6, 24, and 48 hours post-injection), mice were euthanized and tumors were aseptically excised and weighed.

Tumor tissues were processed under sterile conditions to quantify bacterial loads. Excised tumors were homogenized in 1 mL of sterile PBS using sterile pestles in a laminar flow cabinet to prevent contamination. Homogenates were subjected to mechanical agitation at 380 rpm for 20 minutes at 15 °C to ensure complete bacterial release from tissue matrices. Supernatants were collected and serially diluted (10^0, 10^{-1}, 10^{-2}, and 10^{-3}) in sterile PBS.

For bacterial enumeration, 5 μL aliquots of each dilution were plated onto appropriate agar media and incubated for 5 days at room temperature to allow colony development. Bacterial colonies were manually counted using established microbiological techniques, and CFU/gram of tumor tissue was calculated to determine bacterial colonization efficiency and proliferation kinetics within tumor tissues.

Colony assay in blood

Bacterial colony assays in blood samples were performed to assess bacterial pharmacokinetics. Female BALB/c mice received intravenous injections of *E. americana* (200 μL, 5×10^9 CFU/mL). Blood samples were collected from the inferior vena cava of the mice after 5 min, 3 h, 24 h, and 48 h. Each blood sample (100 μL) was inoculated onto an agar plate. After being anaerobically incubated for 1 day, the bacterial colonies that formed were imaged. To count the bacterial colonies, the supernatant was diluted 0, 10, 100, and 1000 times with PBS, and then a sample (5 μL) was inoculated onto an agar plate as mentioned above. Finally, bacterial colonies that formed were manually counted.

Three-dimensional tumor spheroid cytotoxicity assays

To evaluate the direct cytotoxic effects of *E. americana* against cancer cells in a more physiologically relevant model system, three-dimensional tumor spheroid assays were employed. Colon-26 cells were seeded at 1×10^4 cells per well in specialized 3D culture spheroid plates (Cell-able® BP-96-R800; Toyo Gosei Co., Ltd., Tokyo, Japan) according to manufacturer specifications optimized for spheroid formation and maintenance.

Spheroids were cultured for 5 days at 37 °C in a humidified incubator with 5% CO_2 to achieve uniform spheroid formation and maturation. Culture medium was replaced every 48 hours to maintain optimal nutrient conditions and remove metabolic waste products. Upon reaching appropriate size and density,

spheroids were exposed to varying concentrations of *E. americana* (5×10^4, 5×10^5, 5×10^6, 5×10^7, and 5×10^8 CFU) to establish dose-response relationships.

Following bacterial exposure, spheroids were thoroughly washed with sterile PBS to remove non-adherent bacteria and cultured under standard conditions. Spheroid morphology, integrity, and viability were assessed using fluorescence microscopy (IX73 system, Olympus Corporation, Tokyo, Japan) equipped with appropriate mirror units (IRDYE800-33LP-A-U01; Semrock Inc.) and high-resolution objectives (20 × magnification, numerical aperture 0.75; UPLSAPO20X, Olympus). Time-lapse imaging was performed to document spheroid disruption kinetics and bacterial-induced cytotoxic effects over 24-120 hour observation periods.

Quantitative PCR analysis of immune responses

To characterize the immune response mechanisms underlying *E. americana* antitumor activity, comprehensive quantitative PCR (qPCR) analysis was performed to assess immune cell infiltration and cytokine expression profiles within tumor tissues. Female BALB/c mice bearing Colon-26 tumors (approximately 200 mm^3) were administered *E. americana* (200 μL, 1×10^9 CFU) or PBS control via intravenous injection.

At 6 hours post-treatment, a time point selected to capture early immune activation events, mice were humanely euthanized and tumor tissues were immediately harvested and flash-frozen in liquid nitrogen to preserve RNA integrity. Total RNA extraction was performed using established protocols with handheld homogenizers (Thermo Fisher Scientific Inc., Waltham, MA, USA) followed by column-based purification methods to ensure high-quality RNA suitable for quantitative analysis.

qPCR analysis was conducted using a QuantStudio 1 Real-Time PCR System (Thermo Fisher Scientific) with gene-specific TaqMan primer-probe sets designed for optimal specificity and efficiency (Supplementary Table S12). Target genes included markers for immune cell populations: CD3 (T cells), CD19 (B cells), Ly6G (neutrophils), F4/80 (macrophages), and NK cell markers, as well as inflammatory cytokines IFN-γ and TNF-α. ACTB (β-actin) served as the endogenous control gene, measured using TaqMan Array Mouse Endogenous Control plates (Thermo Fisher Scientific).

All reactions were performed in triplicate to ensure statistical reliability, with thermal cycling conditions optimized for TaqMan chemistry: 50 °C for 2 minutes (AmpErase UNG activation), 95 °C for 2 minutes (AmpliTaq Gold DNA polymerase activation), followed by 40 cycles of denaturation at 95 °C for 1 second and annealing/extension at 60 °C for 20 seconds. PCR efficiency validation was performed using 10-fold serial dilutions, achieving efficiencies ranging from 90-100% for all primer sets. Gene expression data were analyzed using the comparative Ct method and presented as fold-change ($\log_{10}$ relative quantification) compared to control groups.

Immunohistochemical analysis of tumor tissues

Comprehensive immunohistochemical (IHC) analysis was performed to visualize and quantify immune cell infiltration patterns within tumor tissues following *E. americana* treatment. Female BALB/c mice bearing Colon-26 tumors (approximately 200 mm^3) were treated with *E. americana* (200 μL, 1×10^9 CFU) or PBS control and euthanized 24 hours post-treatment to capture peak immune cell infiltration.

Tumor tissues were immediately fixed in 10% neutral-buffered formalin for 24-48 hours, followed by standard paraffin embedding procedures performed by Biopathology Institute Co., Ltd. (Oita, Japan) according to established histopathological protocols. Tissue sections were cut at 3-4 μm thickness using precision microtomes and mounted on charged glass slides for immunostaining procedures.

IHC staining protocols employed primary antibodies specific for immune cell markers including CD3 (T cells), CD19 (B cells), and CXCR4 (neutrophils), as well as apoptosis markers including cleaved caspase-3 (Supplementary Table S13). Primary antibody incubations were performed according to optimized protocols with appropriate positive and negative controls to ensure staining specificity and reproducibility. Sections were counterstained with hematoxylin to provide cellular context and examined using high-resolution light microscopy (BZ-X800 system, Keyence Corporation, Osaka, Japan).

Quantitative analysis of positive staining areas was performed using digital microscopy systems equipped with specialized image analysis software (BZ-X800 Analyzer V1.1.2.4, Keyence Corporation). Multiple representative fields were analyzed for each specimen to ensure statistical validity, with quantification performed by trained personnel blinded to treatment conditions to minimize analytical bias.

TUNEL apoptosis detection assay

Terminal deoxynucleotidyl transferase dUTP nick end labeling (TUNEL) assays were performed to detect and quantify apoptotic cell death within tumor tissues following *E. americana* treatment. Paraffin-embedded tumor tissue sections prepared as described above were subjected to TUNEL staining using established protocols with appropriate positive and negative controls. TUNEL-positive cells were quantified using digital microscopy and image analysis systems to determine the extent of treatment-induced apoptosis.

Comprehensive safety and toxicity evaluation

Extensive safety assessments were conducted to evaluate the systemic effects and potential toxicity of *E. americana* administration. Female BALB/c mice (7 weeks old, average body weight 20 g, $n = 5$ per group) were intravenously administered either *E. americana* (200 μL, 1×10^9 CFU) or PBS control via tail vein injection.

Hematological and biochemical analyzes were performed at 1 day, 2 days, 3 days, 10 days, and 30 days post-treatment by certified laboratory facilities (Japan SLC Inc. and Oriental Yeast Co., Ltd., Tokyo, Japan) according to standardized protocols. Blood samples were collected from the inferior vena cava under terminal anesthesia to obtain adequate sample volumes for comprehensive analysis.

Complete blood count (CBC) parameters included white blood cell count (WBC), red blood cell count (RBC), platelet count (PLT), hematocrit (HCT), hemoglobin concentration (HGB), mean corpuscular volume (MCV), mean corpuscular hemoglobin (MCH), and mean corpuscular hemoglobin concentration (MCHC). Biochemical analysis encompassed liver function markers (ALT, AST, ALP, total bilirubin), kidney function indicators (BUN, creatinine), metabolic parameters (glucose, total protein, albumin), and electrolyte balance (sodium, potassium, chloride).

Histopathological examination

For comprehensive organ toxicity assessment, major organs including liver, spleen, heart, lungs, and kidneys were harvested at 30 days post-treatment and subjected to detailed histopathological examination. Organs were fixed in 10% neutral-buffered formalin, processed using standard histological techniques, and sectioned at 4-5 μm thickness. Hematoxylin and eosin (H&E) staining was performed according to established protocols, and sections were examined by qualified veterinary pathologists for evidence of tissue damage, inflammatory infiltration, necrosis, or other treatment-related pathological changes.

Statistical analysis and data presentation

All experiments were conducted with appropriate statistical power based on preliminary studies and established effect sizes. Each experiment included a minimum of three biological replicates ($n \geq 3$) and was independently repeated at least three times to ensure reproducibility and statistical validity. For *in vivo* studies, group sizes of $n = 5$ were employed based on power analysis calculations to detect clinically meaningful differences with 80% power at $\alpha = 0.05$.

Quantitative data are presented as mean ± standard error of the mean (SEM) unless otherwise specified. Statistical analyzes were performed using GraphPad Prism software (version 9.4.0; GraphPad Software Inc., Boston, MA, USA). Comparisons between two groups were analyzed using unpaired Student's t-tests with Welch's correction for unequal variances when appropriate. Multiple group comparisons were analyzed using one-way analysis of variance (ANOVA) followed by Tukey's post-hoc test for pairwise

comparisons. Survival data were analyzed using Kaplan-Meier survival curves with statistical significance determined by log-rank (Mantel-Cox) tests.

For all analyzes, P values < 0.05 were considered statistically significant, with significance levels denoted as follows: $*P < 0.05$, $**P < 0.01$, $***P < 0.001$, and $****P < 0.0001$. All statistical tests were two-tailed unless otherwise specified, and assumptions of normality and equal variances were verified using appropriate diagnostic tests before applying parametric statistical methods.

Disclosure of Potential Conflicts of Interest

The authors declare no competing interests.

Acknowledgments

We thank Mr. Mitsuru Kawahara (JAIST) and Ms. Mariko Deguchi (JAIST) for their dedicated support for the animal experiments.

Author contributions

CRediT: **Seigo Iwata:** Investigation, Formal analysis, Data curation, Validation, Writing – original draft; **Nagi Yamasita**: Investigation, Formal analysis, Data curation, Validation; **Kensuke Asukabe**: Investigation, Formal analysis, Data curation, Validation; **Matomo Sakari:** Software, Formal analysis; **Eijiro Miyako:** Conceptualization, Methodology, Software, Formal analysis, Resources, Data curation, Writing – original draft, Project administration, Funding acquisition, Writing – review & editing, Visualization, Supervision.

Funding

This work was financially supported by Japan Society for the Promotion of Science (JSPS) KAKENHI Grant-in-Aid for Scientific Research (A) (Grant number 23H00551), JSPS KAKENHI Grant-in-Aid for Challenging Research (Pioneering) (Grant number 25K21827), JSPS Program for Forming Japan's Peak Research Universities (J-PEAKS) (Grant number JPJS00420230006), and the Japan Science and Technology Agency (JST) Program for co-creating startup ecosystem (Grant Number JPMJSF2318). S. I. thanks to JST SPRING (Grant number JPMJSP2102).

Data and code availability statement

All data needed to evaluate the conclusions in the paper are presented in the paper and/or the Supplementary Materials. Additional data related to this paper are available from the corresponding author on reasonable request.

ORCID

Eijiro Miyako 0000-0002-1157-6174

References

1. Michaudel C, Sokol H. The Gut microbiota at the service of immunometabolism. Cell Metab. 2020;32(4):514–523. doi: 10.1016/j.cmet.2020.09.004.
2. Quaglio AEV, Grillo TG, Oliveira ECS, Stasi LC, Sassaki LY. Gut microbiota, inflammatory bowel disease and colorectal cancer. World J Gastroenterol. 2022;28(30):4053–4060. doi: 10.3748/wjg.v28.i30.4053.
3. Gensollen T, Iyer SS, Kasper DL, Blumberg RS. How colonization by microbiota in early life shapes the immune system. Science. 2016;352:539–544. doi: 10.1126/science.aad9378.
4. Ting NL, Lau HC, Yu J. Cancer pharmacomicrobiomics: targeting microbiota to optimise cancer therapy outcomes. Gut. 2022;71:1412–1425. doi: 10.1136/gutjnl-2021-326264.
5. Zheng D, Liwinski T, Elinav E. Interaction between microbiota and immunity in health and disease. Cell Res. 2020;30:492–506. doi: 10.1038/s41422-020-0332-7.
6. Dutta D, Lim SH. Bidirectional interaction between intestinal microbiome and cancer: opportunities for therapeutic interventions. Biomark Res. 2020;8:31. doi: 10.1186/s40364-020-00211-6.

7. Karwowska Z, Szemraj J, Karwowski B. Microbiota Alterations in Gastrointestinal Cancers. Appl Sci. 2020;10:585. doi: 10.3390/app10020585.
8. Cullin N, Antunes CA, Straussman R, Stein-Thoeringer CK, Elinav E. Microbiome and cancer. Cancer Cell. 2021;39:1317–1341. doi: 10.1016/j.ccell.2021.08.006.
9. Kaźmierczak-Siedlecka K, Daca A, Fic M, van de Wetering T, Folwarski M, Makarewicz W. Therapeutic methods of gut microbiota modification in colorectal cancer management – fecal microbiota transplantation, prebiotics, probiotics, and synbiotics. Gut Microbes. 2020;11(6):1518–1530. doi: 10.1080/19490976.2020.1764309.
10. Zitvogel L, Daillère R, Roberti M, Routy B, Kroemer G. Anticancer effects of the microbiome and its products. Nat Rev Microbiol. 2017;15:465–478. doi: 10.1038/nrmicro.2017.44.
11. Nobels A, van Marcke C, Jordan BF, Hul MV, Cani PD. The gut microbiome and cancer: from tumorigenesis to therapy. Nat. Metab. 2025;7:895–917. doi: 10.1038/s42255-025-01287-w.
12. Routy B, Le Chatelier E, Derosa L, Duong CPM, Alou MT, Daillère R, Fluckiger A, Messaoudene M, Rauber C, Roberti MP, et al. Gut microbiome influences efficacy of PD-1–based immunotherapy against epithelial tumors. Science. 2018;359:91–97.
13. Mao J, Wang D, Long J, Yang X, Lin J, Song Y, Xie F, Xun Z, Wang Y, Wang Y, et al. Gut microbiome is associated with the clinical response to anti-PD-1 based immunotherapy in hepatobiliary cancers. J Immunother Cancer. 2021;9(12):e003334. doi: 10.1136/jitc-2021-003334.
14. Zheng Y, Wang T, Tu X, Huang Y, Zhang H, Tan D, Jiang W, Cai S, Zhao P, Song R, et al. Gut microbiome affects the response to anti-PD-1 immunotherapy in patients with hepatocellular carcinoma. J. Immunotherapy Cancer. 2019;7(1):193. doi: 10.1186/s40425-019-0650-9.
15. Goto Y, Iwata S, Miyahara M, Miyako E. Discovery of intratumoral oncolytic bacteria toward targeted anticancer theranostics. Adv Sci. 2023;10:23016.
16. Iwata S, Nishiyama T, Sakari M, Doi Y, Takaya N, Ogitani Y, Nagano H, Fukuchi K, Miyako E. Tumour-resident oncolytic bacteria trigger potent anticancer effects through selective intratumoural thrombosis and necrosis. Nat Biomed Eng. 2025:1459. doi: 10.1038/s41551-025-01459-9.
17. Chintalapati SSVV, Iwata S, Miyahara M, Miyako E. Tumor-isolated *Cutibacterium acnes* as an effective tumor suppressive living drug. Biomed Pharmacother. 2024;170:116041. doi: 10.1016/j.biopha.2023.116041.
18. Rommasi F. Bacterial-based methods for cancer treatment: what we know and where we are. Oncol. Ther. 2022;10:23–54. doi: 10.1007/s40487-021-00177-x.
19. Sarotra P, Medhi B. Use of bacteria in cancer therapy. Current strategies in cancer gene therapy. 2017;209:111–121.
20. Miyahara M, Doi Y, Takaya N, Miyako E. Photocatalytic scaffolds enhance anticancer performances of bacterial consortium AUN. Chem Eng J. 2024;499:156378. doi: 10.1016/j.cej.2024.156378.
21. Chintalapati S, Sang N, Miyahara M, Iwata S, Nishida K, Miyako E. Living drugs: a wonderful evolution for therapeutic applications. Cell Biomater. 2025;1:100193. doi: 10.1016/j.celbio.2025.100193.
22. Dieterich W, Schink M, Zopf Y. Microbiota in the Gastrointestinal Tract. Med Sci. 2018;6:116.
23. Sommer F, Backhed F. The gut microbiota-Masters of host development and physiology. Nat Rev Microbiol. 2013;11:227–238.
24. O'Hara AM, Shanahan F. The gut flora as a forgotten organ. EMBO Rep. 2006;7:688–693.
25. Torres-Dimas E, Cruz-Ramírez A, Bermúdez-Cruz RM. Cancer in amphibia, a rare phenomenon? Cell. Biology. International. 2022;46:1992–1998. doi: 10.1002/cbin.11888.
26. Brown J, Wilson W. Exploiting tumour hypoxia in cancer treatment. Nat Rev Cancer 2004;4:437–447.
27. Luo CH, Huang CT, Su CH, Yeh CS. Bacteria-mediated hypoxia-specific delivery of nanoparticles for tumors imaging and therapy. Nano Lett. 2016;16(6):3493–3499. doi: 10.1021/acs.nanolett.6b00262.
28. Ioannou P, Baliou S, Kofteridis D. *Ewingella americana* infections in humans—A narrative review. Antibiotics. 2024;13:559. doi: 10.3390/antibiotics13060559.
29. Esposito S, Miconi F, Molinari D, Savarese E, Celi F, Marchese L, Valloscuro S, Principi N. What is the role of Ewingella americana in humans? A case report in a healthy 4-year-old girl. BMC Infect Dis. 2019;19:386. doi: 10.1186/s12879-019-4021-4.
30. Dong H, Strome S, Salomao D, Tamura H, Hirano F, Flies DB, Roche PC, Lu J, Zhu G, Tamada K, et al. Tumor-associated B7-H1 promotes T-cell apoptosis: A potential mechanism of immune evasion. Nat Med. 2002;8:793–800. doi: 10.1038/nm730.
31. Lee D, Cho M, Kim E, Seo Y, Cha J. PD-L1: from cancer immunotherapy to therapeutic implications in multiple disorders. Mol Ther. 2024;32(12):4235–4255. doi: 10.1016/j.ymthe.2024.09.026.
32. Chatterjee S, Lesniak WG, Gabrielson M, Lisok A, Wharram B, Sysa-Shah P, Azad BB, Pomper MG, Nimmagadda S. A humanized antibody for imaging immune checkpoint ligand PD-L1 expression in tumors. Oncotarget. 2016;7:10215–10227. doi: 10.18632/oncotarget.7143.
33. Xiaoming D, Yang G, Wenyi W. Post-translational regulations of PD-L1 and PD-1: mechanisms and opportunities for combined immunotherapy. Semin Cancer Biol. 2022;85:246–252. doi: 10.1016/j.semcancer.2021.04.002.
34. Nicoletto RE, Ofner CM. Cytotoxic mechanisms of doxorubicin at clinically relevant concentrations in breast cancer cells. Cancer Chemother Pharmacol. 2022;89:285–311. doi: 10.1007/s00280-022-04400-y.

35. Suzuki F, Hashimoto K, Kikuchi H, Nishikawa H, Matsumoto H, Shimada J, Kawase M, Sunaga K, Tsuda T, Satoh K, et al. Induction of tumor-specific cytotoxicity and apoptosis by doxorubicin. Anticancer Res. 2005;25:887–893.
36. Xu L, Xu S, Wang H, Zhang J, Chen Z, Pan L, Wang J, Wei X, Xie H, Zhou L, et al. Enhancing the efficacy and safety of doxorubicin against hepatocellular carcinoma through a modular assembly approach: the combination of polymeric prodrug design, nanoparticle encapsulation, and cancer cell-specific drug targeting. ACS Appl Mater Interfaces. 2018;10(4):3229–3240. doi: 10.1021/acsami.7b14496.
37. Chen J, Bai Y, Xue K, Li Z, Zhu Z, Yu C, Shen S, Qiao P, Luo Y, Dang E, et al. CREB1-driven CXCR4hi neutrophils promote skin inflammation in mouse models and human patients. Nat Commun. 2023;14:5894. doi: 10.1038/s41467-023-41484-3.
38. Aspalter RM, Eibl MM, Wolf HM. Regulation of TCR-mediated T cell activation by TNF-RII. J Leukoc Biol. 2003;74(4):572–582. doi: 10.1189/jlb.0303112.
39. Liu Y, Wang Y, Yang Y, Weng L, Wu Q, Zhang J, Zhao P, Fang L, Shi Y, Wang P. Emerging phagocytosis checkpoints in cancer immunotherapy. Sig Transduct Target Ther. 2023;8:104. doi: 10.1038/s41392-023-01365-z.
40. Huang C-Y, Ye Z-H, Huang M-Y, Lu J-J. Regulation of CD47 expression in cancer cells. Transl Oncol. 2020;13:100862. doi: 10.1016/j.tranon.2020.100862.
41. Dang LH, Bettegowda C, Huso DL, Kinzler KW, Vogelstein B. Combination bacteriolytic therapy for the treatment of experimental tumors. Proc Natl Acad Sci USA. 2001;98(2010):15155–15160. doi: 10.1073/pnas.251543698.
42. Kawai T, Akira S. The role of pattern-recognition receptors in innate immunity: update on Toll-like receptors. Nat Immunol. 2010;11(2010):373–384. doi: 10.1038/ni.1863.
43. Coffelt SB, Wellenstein MD, de Visser KE. Neutrophils in cancer: neutral no more. Nat Rev Cancer. 2026;16:431–446. doi: 10.1038/nrc.2016.52.
44. Sharma P, Hu-Lieskovan S, Wargo JA, Ribas A. Primary, adaptive, and acquired resistance to cancer immunotherapy. Cell. 2017;168(2017):707–723. doi: 10.1016/j.cell.2017.01.017.
45. Zheng JH, Nguyen VH, Jiang S, Park S, Tan W, Hong SH, Shin MG, Chung I, Bom H, Choy HE, et al. Two-step enhanced cancer immunotherapy with engineered Salmonella typhimurium secreting heterologous flagellin. Sci Transl Med. 2017;9 eaak9537. 10.1126/scitranslmed.aak9537.
46. Type Strains Genome Database. Available from: https://gctype.wdcm.org/.